



# $\Xi_c^0$ production vs multiplicity via hadronic decay in pp@ 13 TeV

Tao Fang<sup>1</sup>, Jianhui Zhu<sup>2,1</sup>, Zhongbao Yin<sup>1</sup>

1, Central China Normal University, China

2, INFN Padova, Italy

# Outline

---

- **Motivation of the analysis**
- **Data sample and event selection**
- **Analysis strategy**
  - Machine learning training and testing
  - Raw yield extraction
  - Efficiency calculation
  - Cross-section
- **Systematic uncertainties**
- **Summary and outlook**

# Motivation

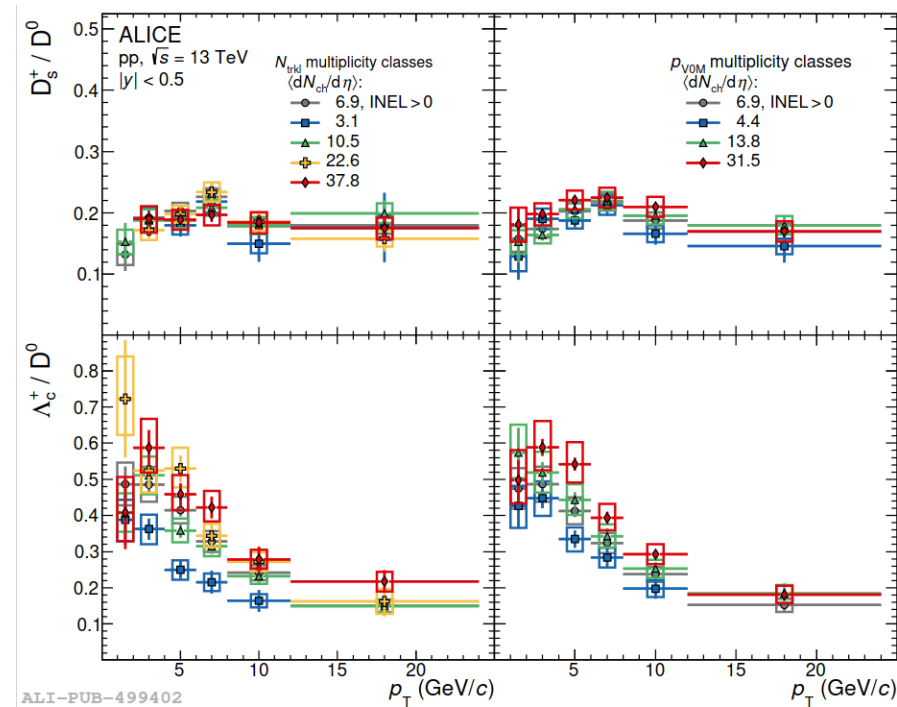
The heavy-flavour production cross section can be calculated as a convolution of three factors

- the parton distribution functions (PDFs)
- the partonic cross section calculated with perturbative QCD calculations
- the fragmentation functions (FFs).

The pre-measurements of the baryon-to-meson  $\Lambda_c^0/D^0$  and  $\Xi_c^{0,+}/D^0$  cross section ratios in pp collisions are inconsistent with measurements in  $e^+e^-$  and ep collision

The  $p_T$ -differential yield ratio of  $\Lambda_c^+/D^0$  shows a significant multiplicity dependence. (right)

The measurement of the multiplicity dependence of  $\Xi_c^0/D^0$  yield ratio can provide further constraints on the study of charm hadronization.



"Phys.Lett.B 829 (2022) 137065"

# Data samples

## MC sample

**MB:** LHC19g6f3\_XcP8\_2016, LHC19g6f2\_XcP8\_2017  
LHC19g6f1\_XcP8\_2018

**HM:** LHC20k7a2\_HMV0M\_18\_p8, LHC20k7b\_HMV0M\_17\_p8  
LHC20k7c\_HMV0M\_16\_p8 (general D2H productio)

## Data sample(Run 2)

- LHC2016 AOD208 kl 13TeV
- LHC2016 AOD208 deghjop 13TeV
- LHC2017 AOD208 cefhijklmor 13TeV
- LHC2018 AOD208 bdefghijklmnop 13TeV

## Event selection

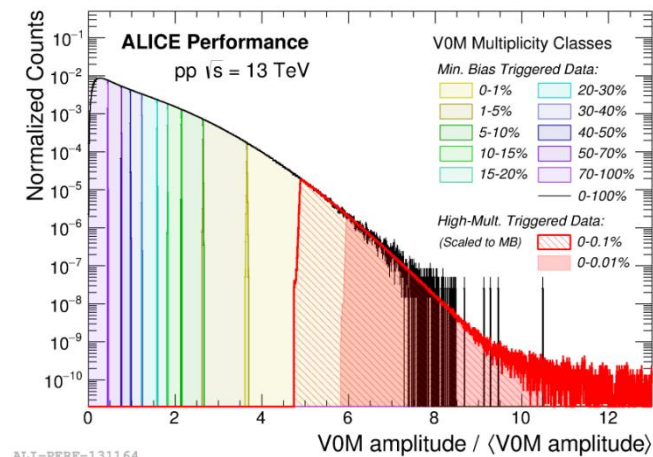
- Trigger Class:
  - kINT7 : MB
  - kHighMultV0 : HMV0
- Pileup rejection only for real data
- Primary vertex Z < 10 cm

## Multiplicity

The selected events are grouped by multiplicity which is based on V0M percentile

$V0M_{pre}[\%]$	$\langle dN_{ch}/d\eta \rangle$	trigger	trigger efficiency	number event
[0.1-30]+INEL > 0	13.81	MB	$0.92 \pm 0.003$	$5.1 \times 10^8$
[30-100]+INEL > 0	4.41	MB	$0.897 \pm 0.013$	$1.34 \times 10^9$
[0-100]+INEL > 0	6.93	MB	$0.997 \pm 0.001$	$1.86 \times 10^9$
[0-0.1]+INEL > 0	31.53	HMV0M	$1.0 \pm 0.0$	$4.60 \times 10^8$

**Table 6:** The table showing V0M percentile multiplicity bins, the average charged particle density  $\langle dN_{ch}/d\eta \rangle$ , the trigger used, trigger efficiency, and number of events.



# Analysis strategy

1. Reconstruction of  $\Xi_c^0 \rightarrow \pi^+ + \Xi^- \rightarrow \pi^+(\pi^-\Lambda) \rightarrow \pi^+(\pi^-(p\pi^-))$  use Kalman Filter (KF) package
2. Use pre-selection and ML to separate of signal and background
  - ML training using XGBoost (integrated in [hipe4ml](#) package)
3. Extract raw yield via invariant mass fit
4. Efficiency calculation from MC
  - $p_T$  re-weight
  - Mult. re-weight
5. Per-event yields calculation
6. Systematics



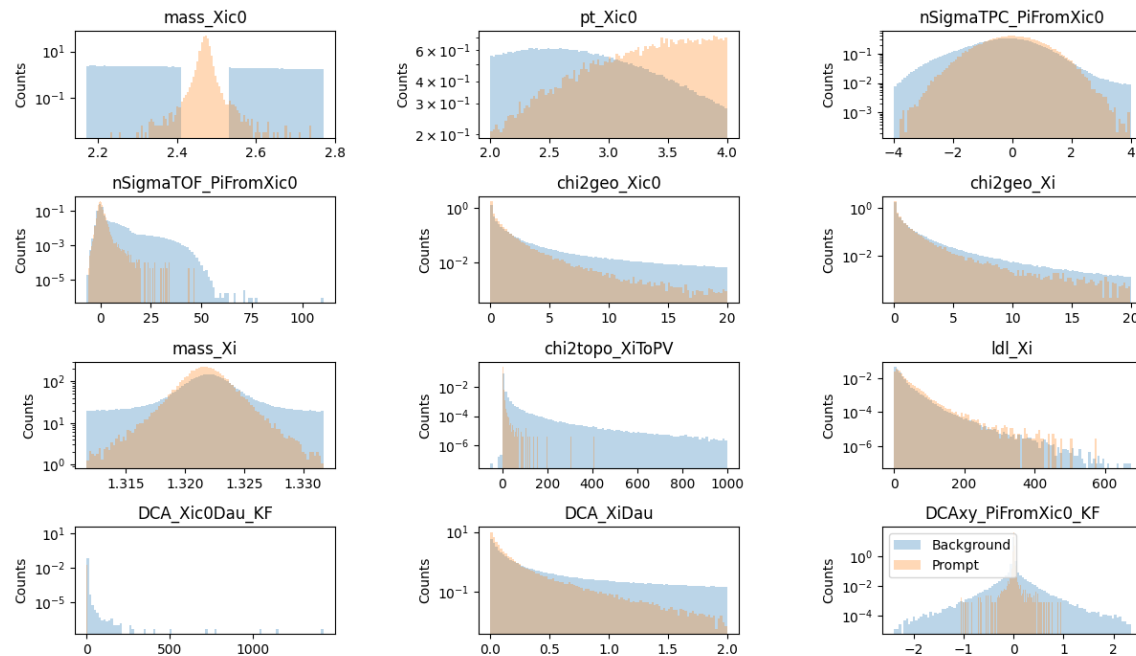
Cuts variables	Cuts
AOD filter bit	4 (Standard cuts with very loose DCA)
Number of TPC crossed rows	> 70
TPC cross rows / findable ratio	> 0.8
Number of TPC clusters for $dE/dx$	> 50
$\chi^2$ /NDF of momentum fit	< 5
Number of points in ITS	> 3

$p_T^{\Xi_c^0}$ (GeV/c)	(2, 4)	(4, 6)	(6, 8)	(8, 12)
$p_T^{\pi^+\Xi_c^0}$ cut	1.0	1.0	0.4	0.4

Cuts variables	Cuts
Number of TPC crossed rows	> 70
TPC cross rows / findable ratio	> 0.8
Number of TPC clusters for $dE/dx$	> 50

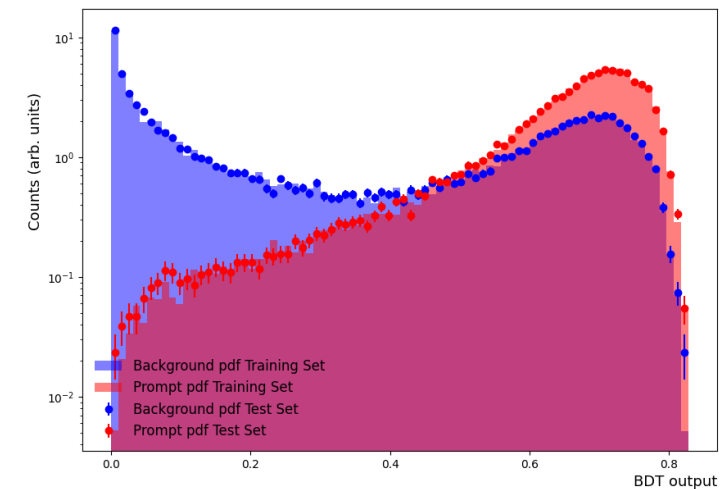
ML is able to handle complex data, make predictions, automate processes

$$2 < p_T < 4 \text{ GeV}/c$$



**training\_columns:** [nSigmaTPC\_PiFromXic0, nSigmaTOF\_PiFromXic0, chi2geo\_Xic0, chi2geo\_Xi, mass\_Xi, chi2topo\_XiToPV, ldl\_Xi, DCA\_Xic0Dau\_KF, DCA\_XiDau, DCAxy\_PiFromXic0\_KF]

## BDT distribution



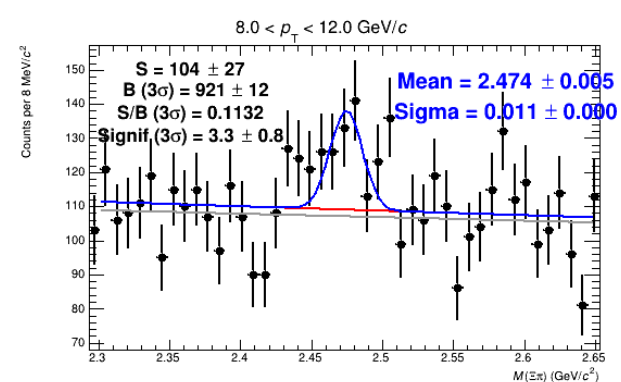
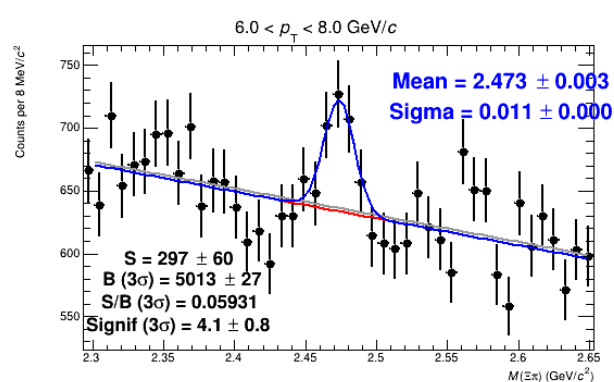
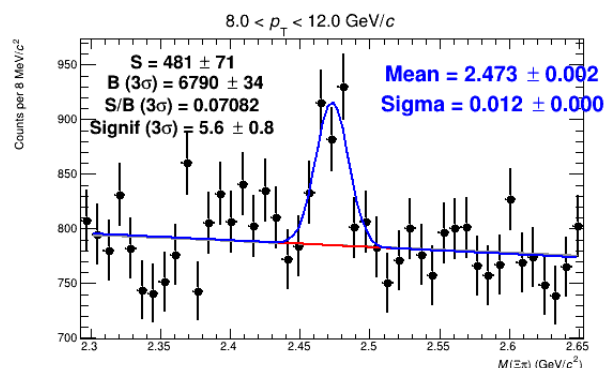
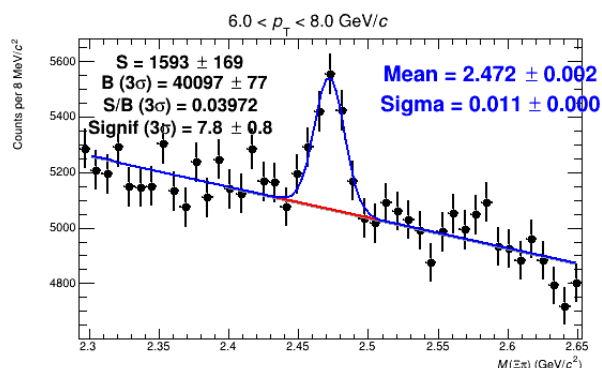
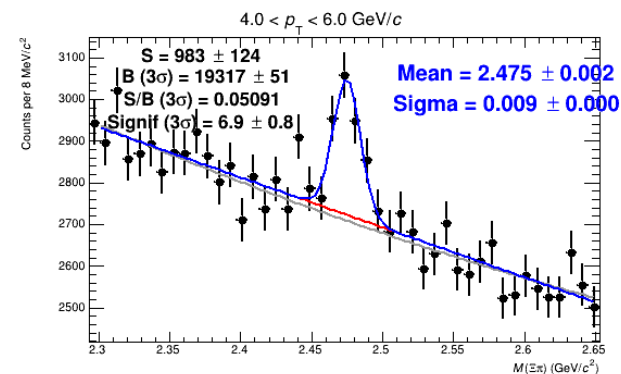
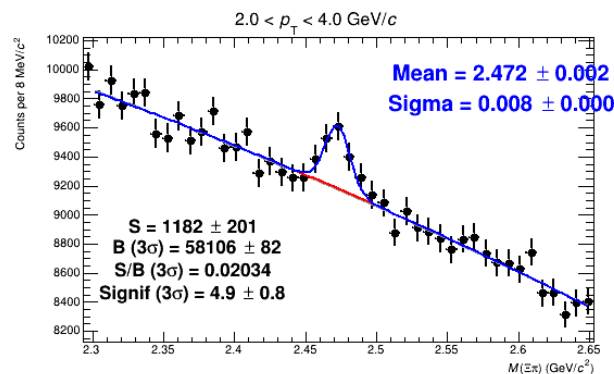
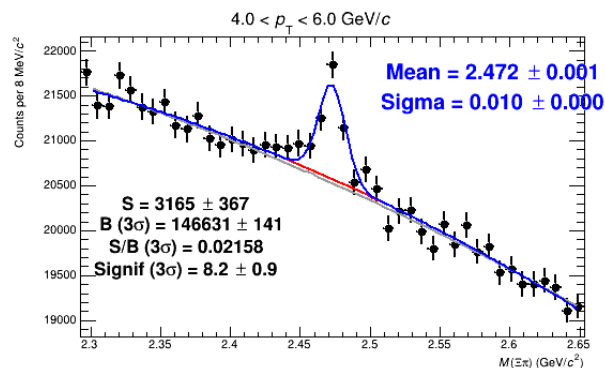
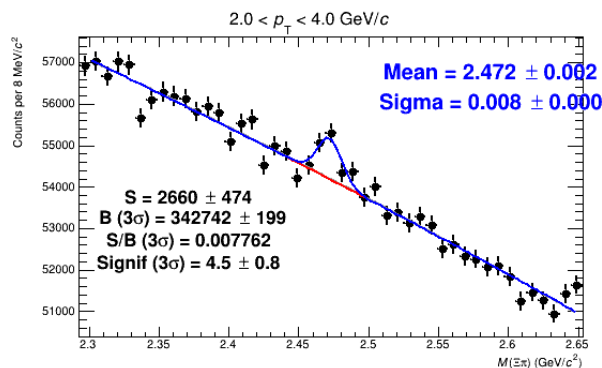
The distribution indicates the contribution and relative importance of each tree to the final model

# Invariant mass

Fit function

**Signal:** Gaussian

**Bkg:** Pol2 for [2-4] & [4-6], Pol1 for [6-8] & [8-12]



HM [0-0.1]

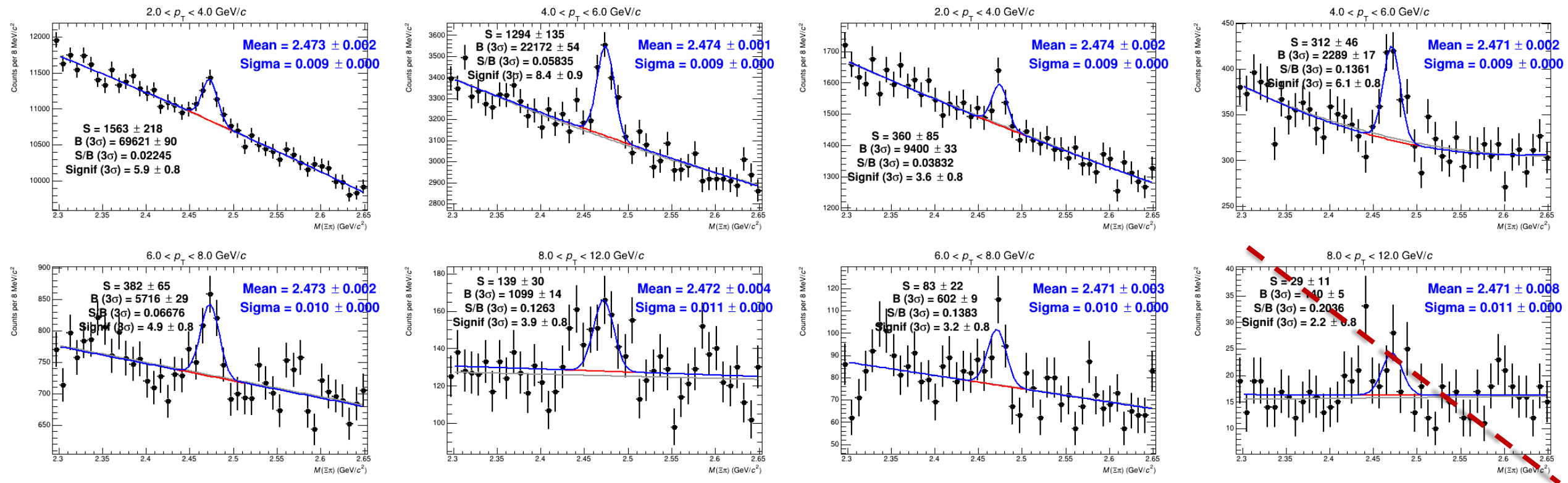
MB [0.1-30]

# Invariant mass

Fit function

**Signal:** Gaussian

**Bkg:** Pol2 for [2-4] & [4-6], Pol1 for [6-8] & [8-12] (not include in MB[30-100])



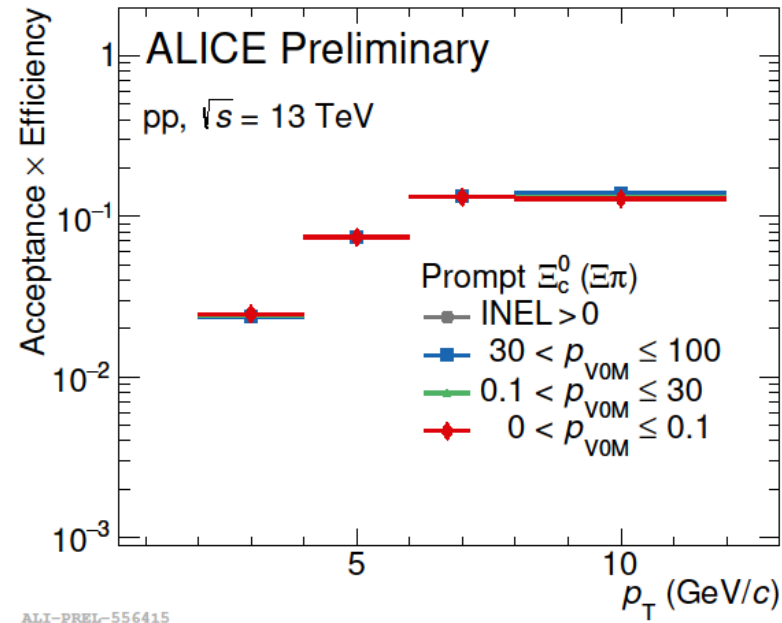
MB [0-100]

MB [30-100]



# Acceptance-times-efficiency

The different pt and multiplicity bin were corrected by reconstruction and selection efficiency as well as acceptance



Prompt accept-times-efficiency of V0M percentile multiplicity bin as function of pt

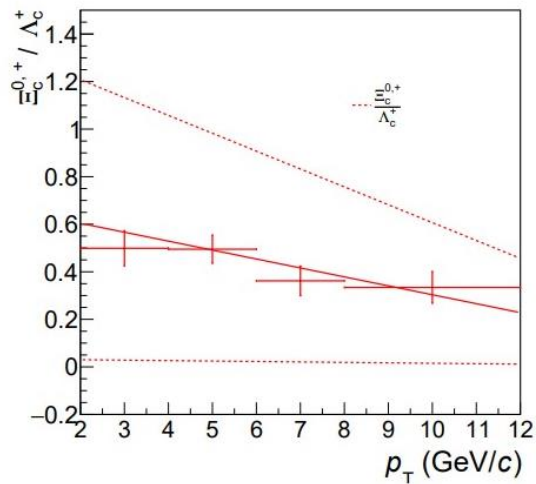
# Feed-Down correction

$$f_{prompt} = 1 - \frac{N_{\Xi_c^0 \text{ from } b}}{N_{\Xi_c^0, raw}} = 1 - \frac{1}{N_{\Xi_c^0, raw}} \cdot \left( \frac{d^2\sigma}{dp_T dy} \right)_{b \rightarrow X \rightarrow \Xi_c}^{theory} \cdot 2 \cdot (Acc * \varepsilon)_{feed-down} \cdot \Delta p_T \cdot \Delta y \cdot BR \cdot L_{int}$$

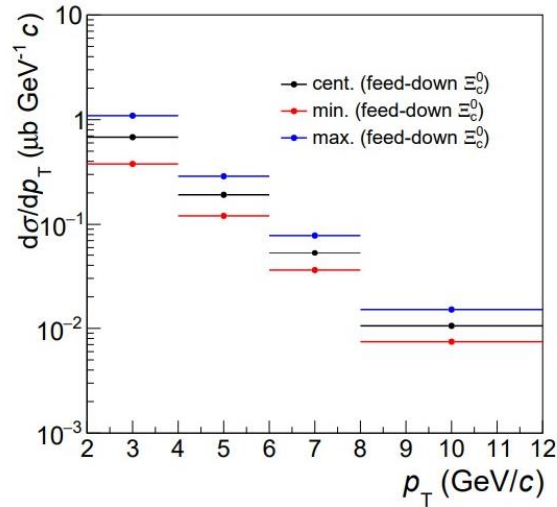
$$\begin{aligned} \left( \frac{d^2\sigma}{dp_T dy} \right)_{b \rightarrow X \rightarrow \Xi_c}^{theory} &= \left( \frac{d^2\sigma}{dp_T dy} \right)_{b \rightarrow X \rightarrow \Lambda_c}^{FONLL} * \left( \frac{\sum_{H_b} F(b \rightarrow H_b \rightarrow \Xi_c)}{\sum_{H_b} F(b \rightarrow H_b \rightarrow \Lambda_c)} \right) \\ &\approx \left( \frac{d^2\sigma}{dp_T dy} \right)_{b \rightarrow X \rightarrow \Lambda_c}^{FONLL} * \frac{c \rightarrow \Xi_c}{c \rightarrow \Lambda_c} \end{aligned}$$

Assumption:

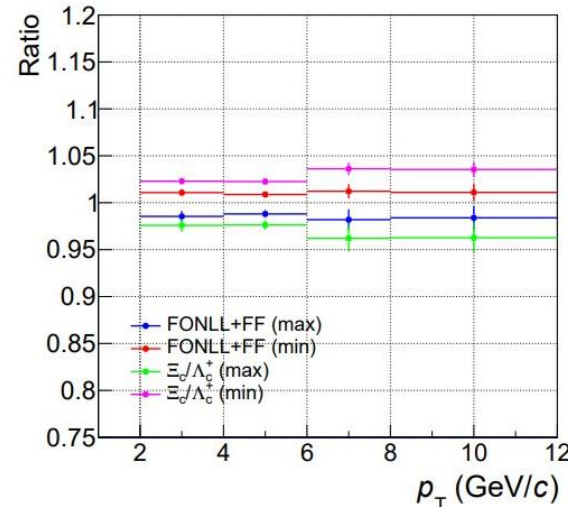
- The  $b \rightarrow \Lambda_b \rightarrow \Lambda_c$  and  $b \rightarrow \Xi_b \rightarrow \Xi_c$  dominant
- The ratio of  $\Xi_c^0/\Lambda_c$  is constant for both inclusive and feed-down baryons.



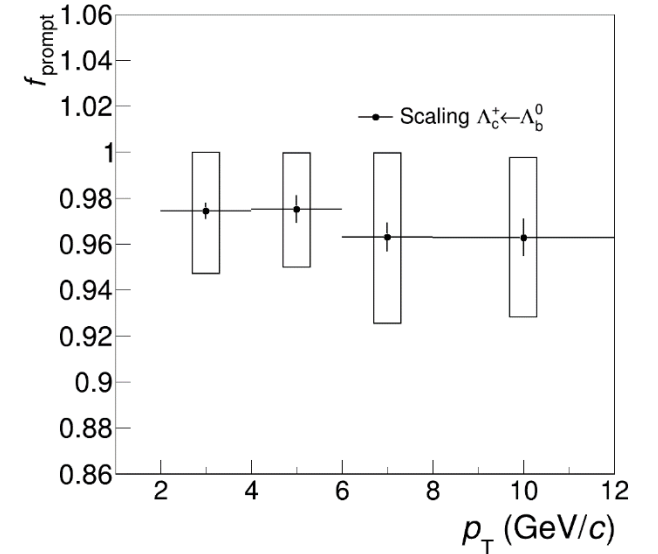
The ratio  $\Xi_c$  of over  $\Lambda_c$  uncertainty



The cross section of feed-down  $\Xi_c^0$  obtained with the scaling procedure



Different scan method



systematic uncertainty for the prompt  $\Xi_c^0$

# Systematic uncertainty

$\Xi_c^0 \rightarrow \pi^+ \Xi^- \rightarrow \pi^+ (\pi^- \Lambda) \rightarrow \pi^+ (\pi^- (p \pi^-))$	$p_T$ interval(GeV/c)			
[0-100]	(2, 4)	(4, 6)	(6, 8)	(8, 12)
Raw Yield	6%	6%	8%	10%
Tracking	5%	5%	5%	8%
BDT	8%	6%	7%	4%
MC $p_T$	3%	1%	0%	0%
Multiplicity weight	0%	0%	1%	1%
Prompt fraction	2%	2%	3%	3%
Prompt fraction(mult. dep.)	-	-	-	-
[30-100]	(2, 4)	(4, 6)	(6, 8)	(8, 12)
Raw Yield	8%	12%	6%	-
Tracking	5%	5%	5%	-
BDT	12%	10%	8%	-
MC $p_T$	3%	1%	0%	-
Multiplicity weight	0%	0%	0%	-
Prompt fraction	2%	2%	3%	-
Prompt fraction(mult.dep.)	2%	2%	2%	-

[0.1-30]	(2, 4)	(4, 6)	(6, 8)	(8, 12)
Raw Yield	8%	6%	10%	10%
Tracking	5%	5%	5%	8%
BDT	6%	4%	7%	8%
MC $p_T$	3%	1%	0%	0%
Multiplicity weight	0%	0%	1%	1%
Prompt fraction	2%	2%	3%	3%
Prompt fraction(mult. dep.)	1%	1%	2%	3%
[0-0.1]	(2, 4)	(4, 6)	(6, 8)	(8, 12)
Raw Yield	10%	12%	10%	6%
Tracking	5%	5%	5%	8%
BDT	6%	4%	10%	6%
MC $p_T$	3%	1%	0%	0%
Multiplicity weight	0%	0%	0%	0%
Prompt fraction	2%	2%	3%	3%
Prompt fraction(mult. dep.)	2%	2%	2%	3%

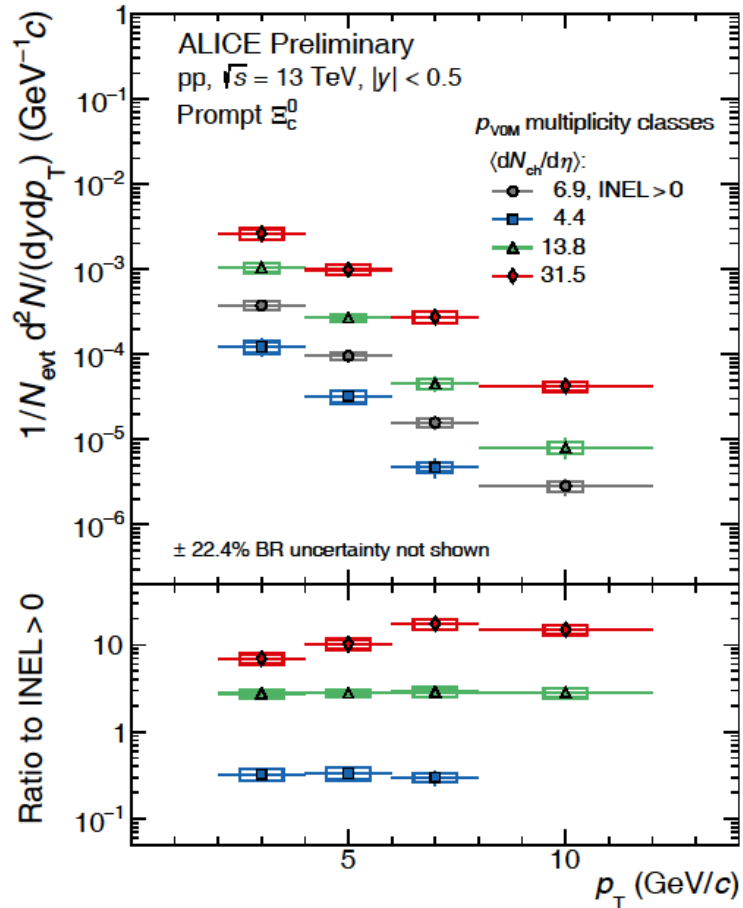
**Table 17:** The systematic uncertainties for  $\Xi_c^0$  in each  $p_T$  bin. (22.4% uncertainties of branch ratio not show)

Systematics  $\Xi_c^0 \rightarrow \pi^+ \Xi^- \rightarrow \pi^+ (\pi^- \Lambda) \rightarrow \pi^+ (\pi^- (p \pi^-))$  for VOM percentile estimator (except for branching ratio  $\pm 22.38\%$  )

More detail in backup

# $p_T$ spectra of $\Xi_c^0$ in different mult.

$$\frac{1}{N_{mult}} \frac{dN_{mult}^{hadron}}{dp_T} = \frac{1}{N_{mult}} \frac{1}{\Delta p_T} \frac{1}{BR_{channel}} \frac{f_{prompt} \epsilon_{trigger} N_{mult}^{hadron, raw}}{2y_{fid}(Acc \times \epsilon)_{prompt}}$$

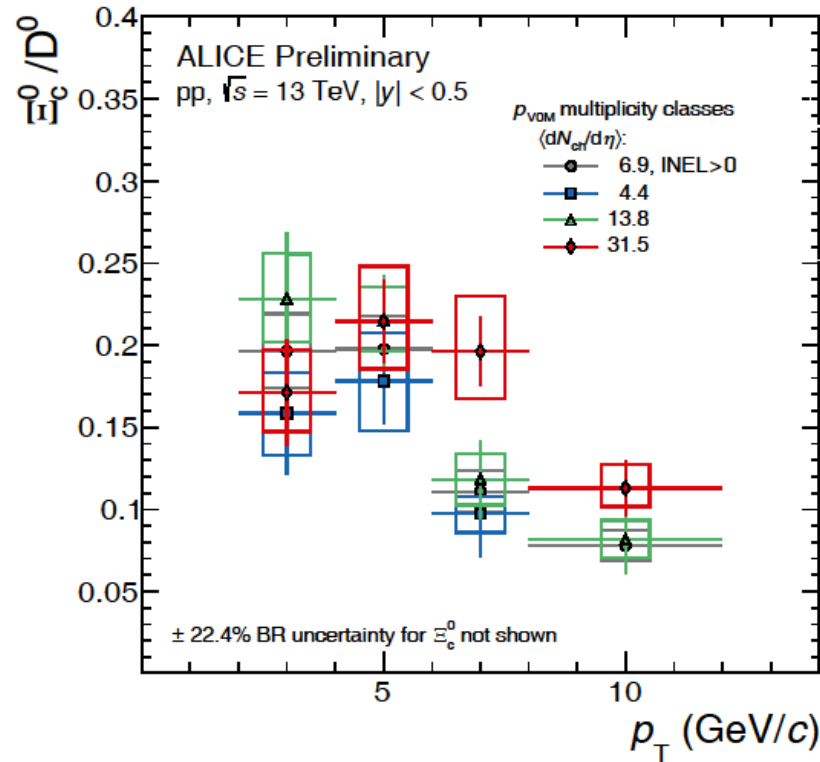


$p_T$  spectra of  $\Xi_c^0$  measured in different multiplicity classes selected with VOM at forward rapidity.

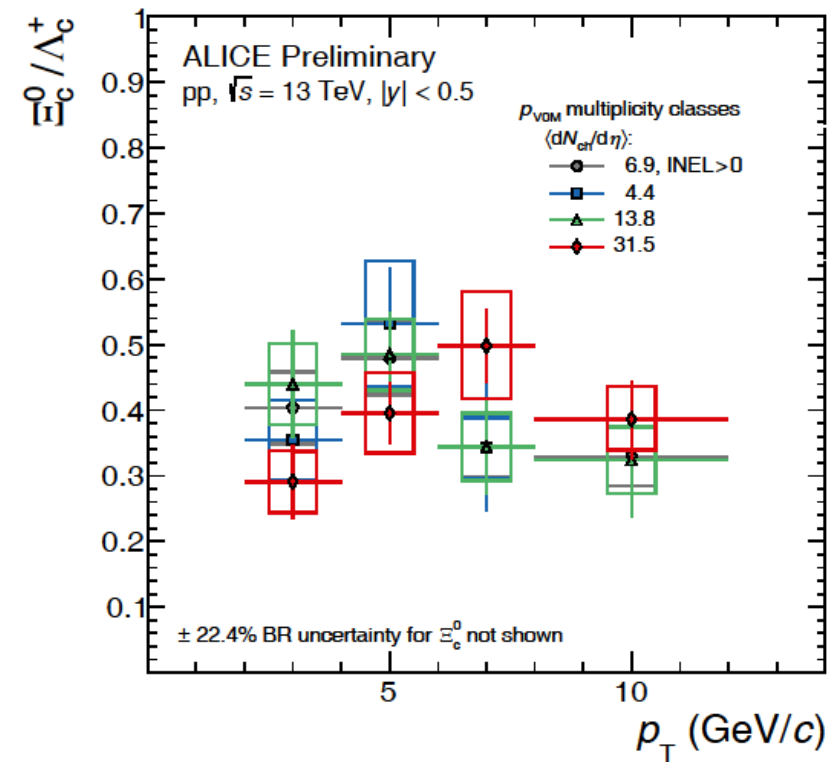
The corresponding ratios to inelastic collisions event with at least one charged particle in the pseudorapidity range  $|\eta| < 1$  (INEL > 0)

# $\Xi_c^0/D^0$ and $\Xi_c^0/\Lambda_c^+$

The  $\Xi_c^0/D^0$  and  $\Xi_c^0/\Lambda_c^+$  ratios at different multiplicity classes in pp collisions



ALI-PREL-548903

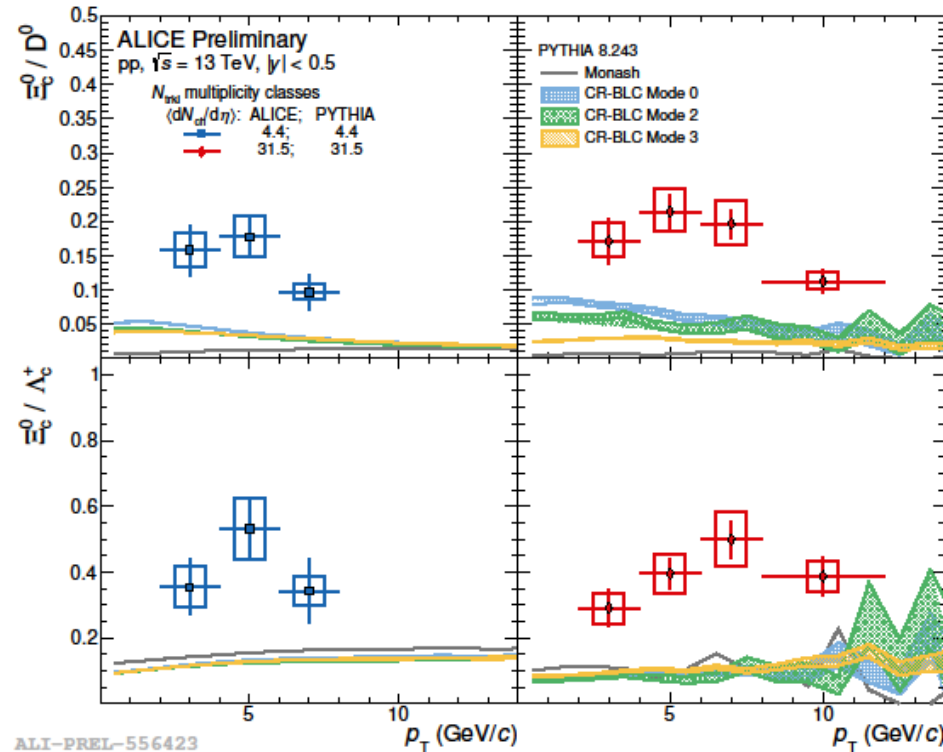


ALI-PREL-548906

The multiplicity dependence of  $\Xi_c^0/D^0$  and  $\Xi_c^0/\Lambda_c^+$  is not observed with the current uncertainties

# $\Xi_c^0/D^0$ and $\Xi_c^0/\Lambda_c^+$ compared to PYTHIA

The  $\Xi_c^0/D^0$ (top) and  $\Xi_c^0/\Lambda_c^+$ (bottom) ratios measured in pp collisions for the lowest(left) and highest (right) multiplicity. The measurements are compared to PYTHIA 8 predictions with the Monash estimated in similar multiplicity classes.



The Monash and CR-BLC tune does not reproduce the  $\Xi_c^0/D^0$  and  $\Xi_c^0/\Lambda_c^+$  ratio, and the Model does not show a multiplicity dependence.

# Summary

---

## **Done:**

The first measurement of  $\Xi_c^0/D^0$  and  $\Xi_c^0/\Lambda_c^+$  ratios as a function of charged-particle multiplicity in pp collisions at  $\sqrt{s} = 13$  TeV. The  $p_T$ -differential  $\Xi_c^0/D^0$  and  $\Xi_c^0/\Lambda_c^+$  yield ratio does not show a strong multiplicity dependence as function of  $p_T$  with the uncertainties.

## **Next:**

More precise measurements with the data sample collected during the Run 3 of the LHC will allow us to further investigate the shape of the  $p_T$ -integrated baryon-to-meson ratios versus multiplicity, extending the multiplicity reach to lower and higher multiplicity intervals.

The background of the slide is a photograph of a library interior. It features tall, curved wooden bookshelves filled with books. The lighting is soft, and the perspective is from within the aisles, looking up at the shelves. A solid blue horizontal band is superimposed over the middle of the image, containing the text.

Back up



# Mult. weight

MC weight obtained by following step

1. Full event on MC and Data
2. Event selection in MC and Data at last one  $\Xi_c^0$  candidate and require invariant mass off the PDG value 2 sigma (2.452, 2.488) GeV/c
3. Normalize Ntrack for Data and MC
4. Divide from Data by MC to obtain event weight in each multiplicity bin

$$(Acc * \epsilon)(\Delta p_T)^{prompt, mult} = \frac{\sum_i N_{sel,i}(\Delta p_T) \omega_i^{mult}}{\sum_i N_{gen,i}(\Delta p_T) \omega_i^{mult}}$$

$N_{sel,i}$ : Selected number of prompt

$N_{gen,i}$ : Generated number of prompt

Example in  $p_{VOM}[0.1, 30]$

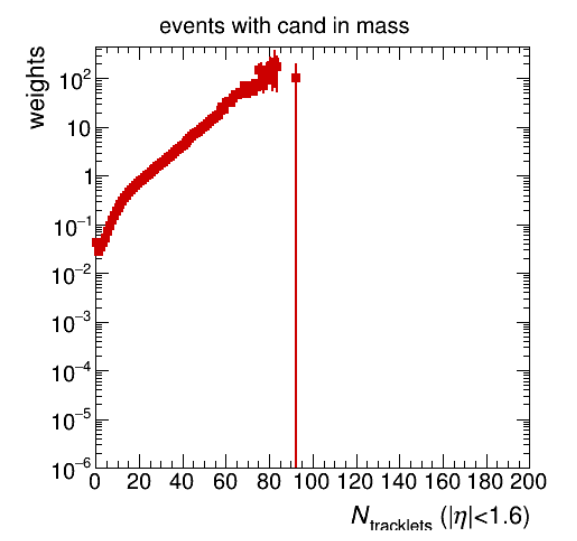
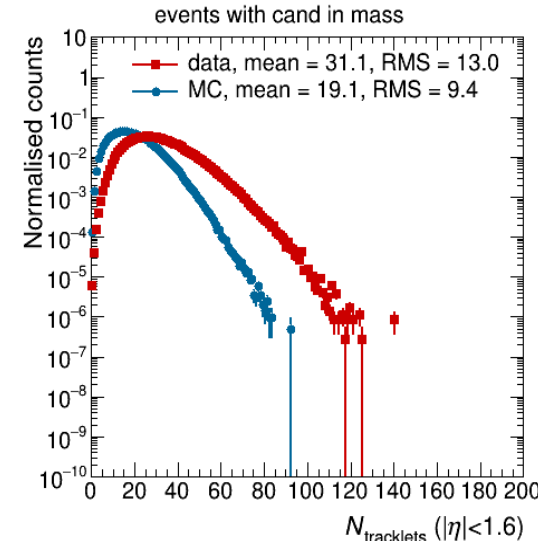
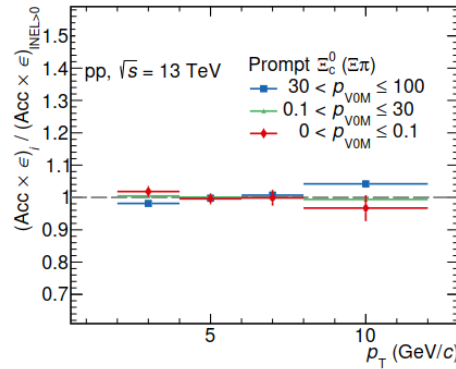
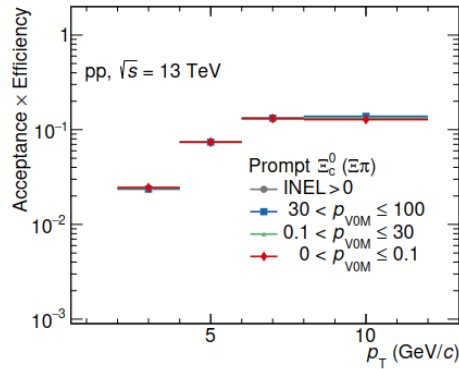
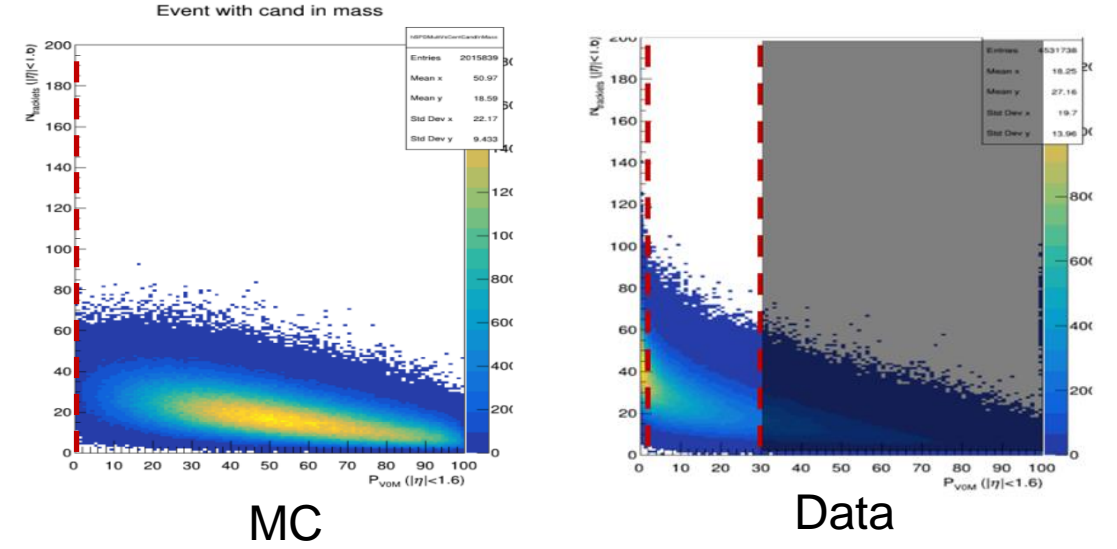


**Fig. 38:** Prompt acceptance-times-efficiency of VOM percentile multiplicity bins as a function of  $p_T$  for  $\Xi_c^0$  per multiplicity interval, The left panels show the ratio with the minimum bias efficiency

# Raw yield extraction

The systematic uncertainties on the raw yield extraction are estimated with a multi-trial approach

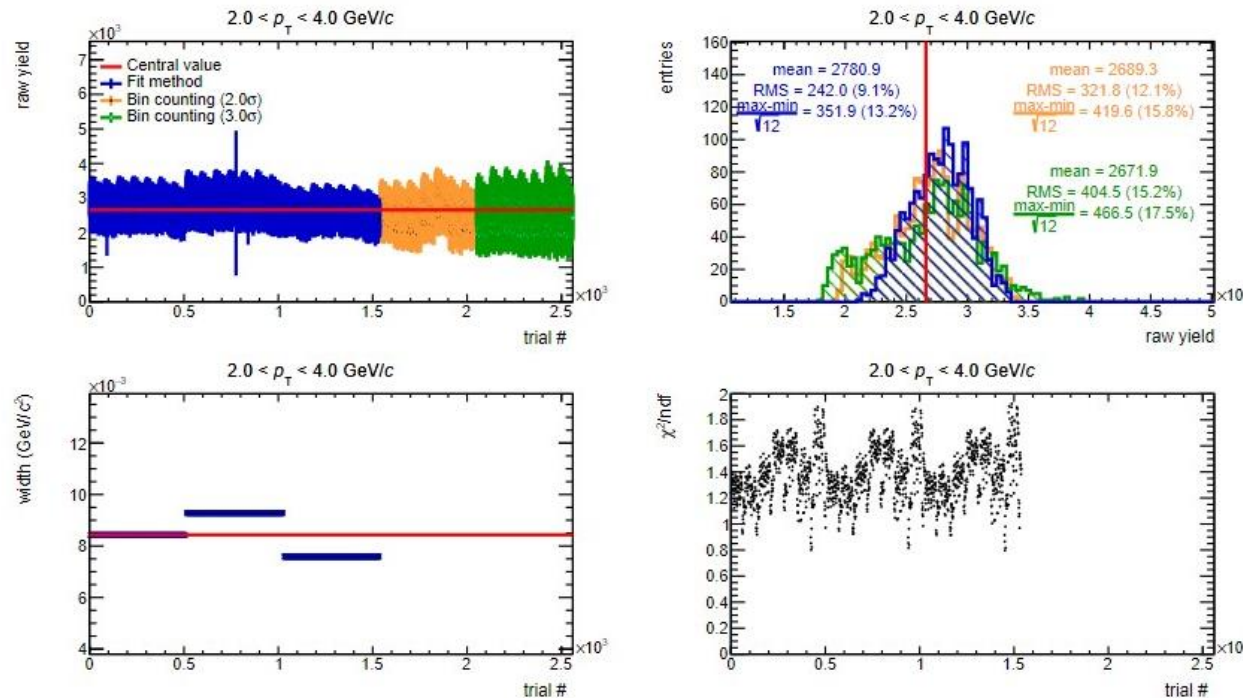


Fig. 30: Raw yield systematic for  $p_T$  bin 2GeV/c-4GeV/c and [0,0.1]V0M percentile multiplicity

## Fit configurations

- Sigma variation: 10%
- Background fit function: lin, expo, pol2
- Mass mins: 2.26, 2.28, 2.30, 2.32, 2.34
- Mass maxs: 2.61, 2.63, 2.65, 2.67, 2.69
- Rebins: 4, 5, 6, 7, 8, 9, 10

- Systematics evaluated as:

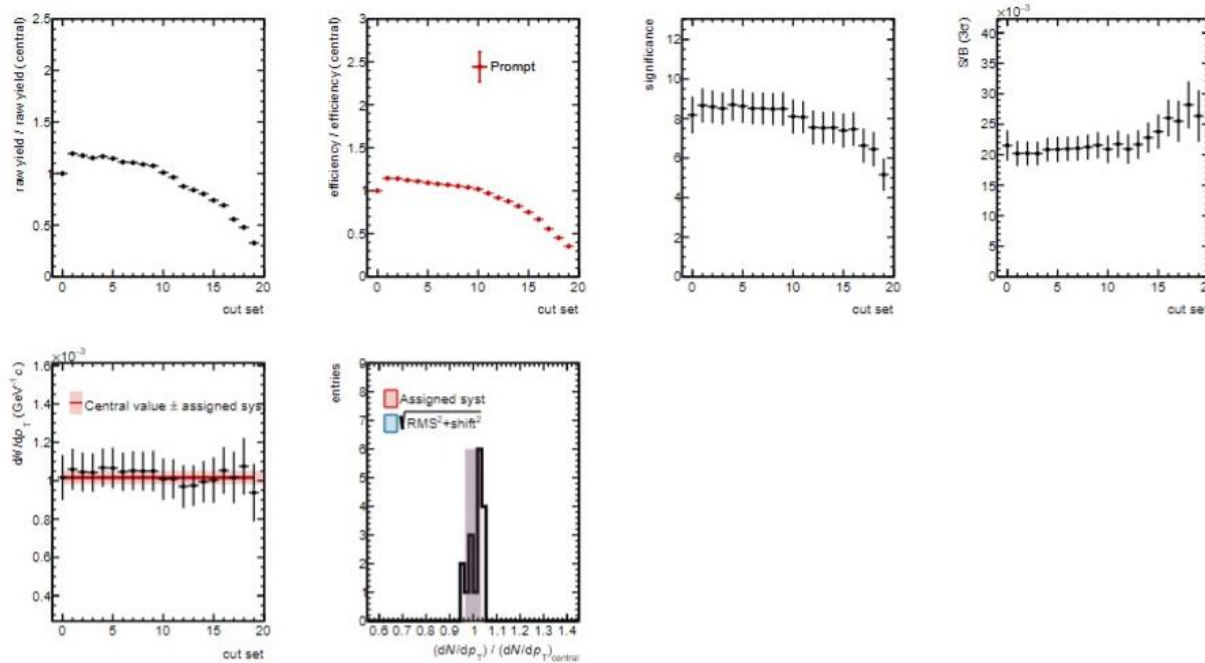
$$\sqrt{\text{RMS}^2 + \text{shift}^2}$$

Assigned systematics range from 6% to 12%

more detailed information is in backup

# BDT selection

Test the effect of the applied selections by varying in a given range.



Trial contributes to systematic if

- Prompt efficiency variation < 35%  
(approximately  $\pm 0.2$  from the working point)
- Significance > 2.5
- $\chi^2 < 2$

Systematics evaluated as:

$$\sqrt{\text{RMS}^2 + \text{shift}^2}$$

Assigned systematics range from 4% to 10%

**Fig. 43:** The cut-variation studies for  $p_T$  bin 4GeV/c-6GeV/c and [0,0.1]V0M percentile multiplicity

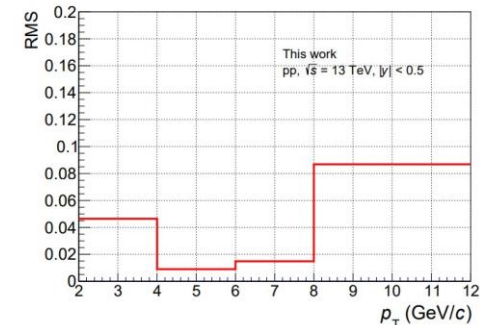
more detailed information is in backup

# Tracking efficiency

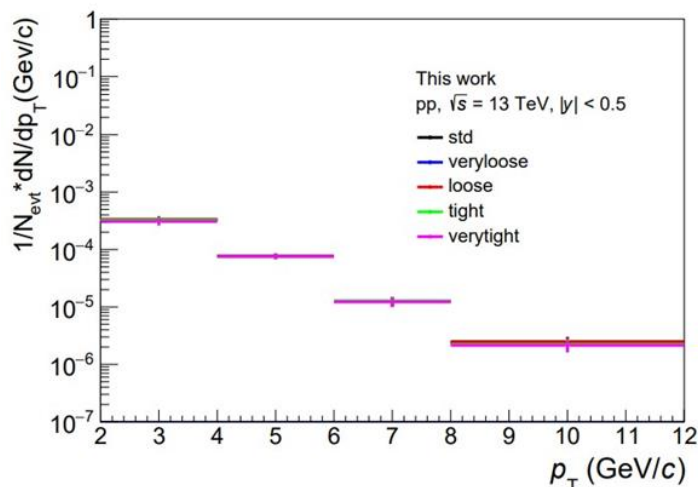
The systematic of tracking in the pre-selection before creating the tree for machine learning  
The TPC applied cuts are shown in

Cuts variables	Very loose	Loose	Standard	Tight	Very tight
Number of TPC crossed rows	> 65	> 70	> 70	> 75	> 80
TPC crossed rows / findable ratio	> 0.75	> 0.75	> 0.80	> 0.85	> 0.90
Number of TPC clusters for $dE/dx$	> 40	> 45	> 50	> 55	> 60

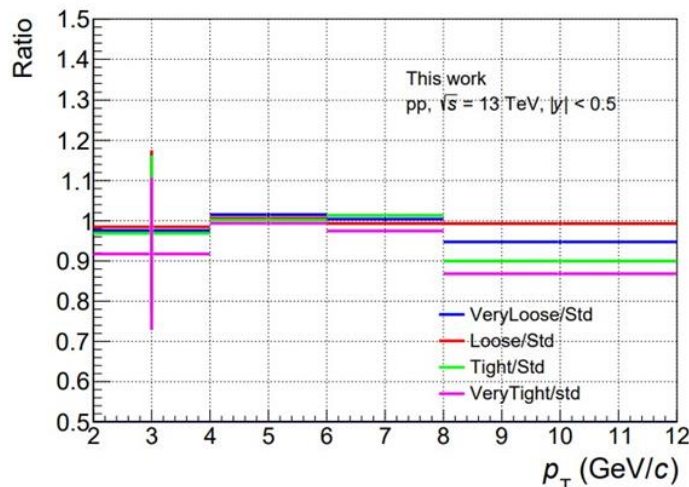
**Table 11:** The variations of TPC parameters in the pre-selection.



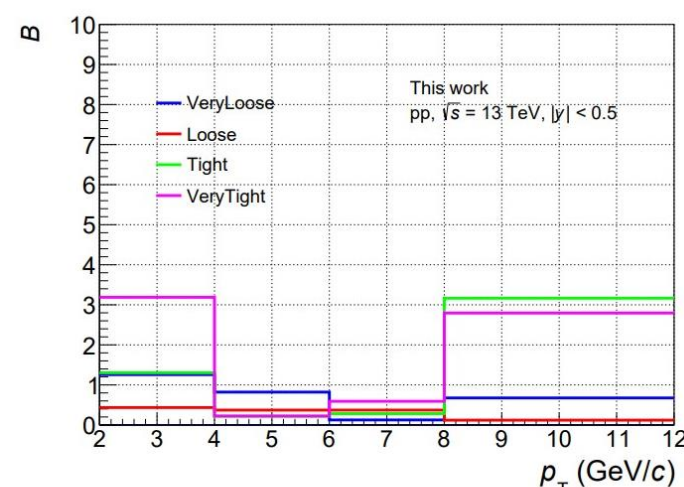
(d) RMS of deviations from 1.



(a)  $\Xi_c^0$   $p_T$  spectrum with different cuts.



(b) The ratio with different cuts to the standard one.



(c) Barlow value for each  $p_T$  bin.

Assigned systematics 5% according ratio of corrected yield



# Working point evaluation

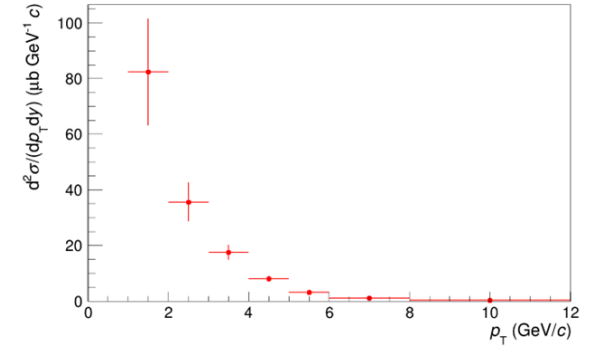
The choice of the ML output scores is performed by guarantees a sufficiently sedu-significance and a sufficiently selection efficiency.

1. Calculate the yield of **background (B)** in  $(-3\sigma_{MC}, 3\sigma_{MC})$ :  
take 10% fraction of data to reduce the effect of statistical fluctuation, fit side bands with “pol1”
2. Calculate the yield of **signal (S)** in  $(-3\sigma_{MC}, 3\sigma_{MC})$ :  
use the published cross section and correct it by acceptance  $\times$  efficiency.

$$S_{expect} = 2 \cdot \left( \frac{d\sigma^2}{dp_T dy} \Big|_{pp} \right) \cdot (Acc \times \varepsilon)_{prompt} \cdot \Delta y \cdot \Delta p_T \cdot BR \cdot L_{int} / f_{prompt}$$

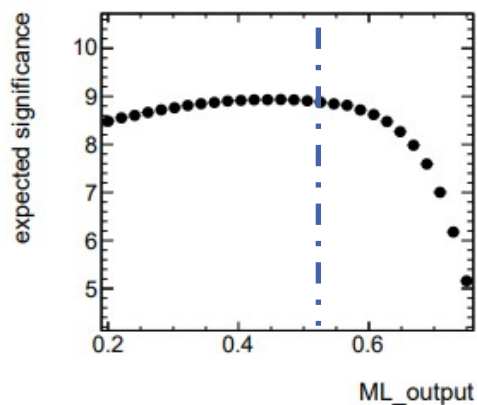
3. Calculate the significance  $S/\sqrt{(S+B)}$

Published Xic0 crossection

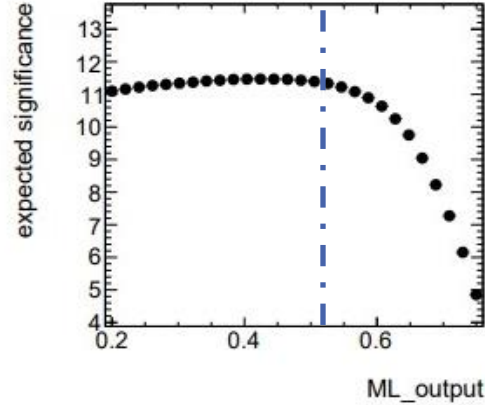


$p_T^{\Xi_c^0}$ (GeV/c)	(2, 4)	(4, 6)	(6, 8)	(8, 12)
BDT cut	0.52	0.5	0.42	0.38

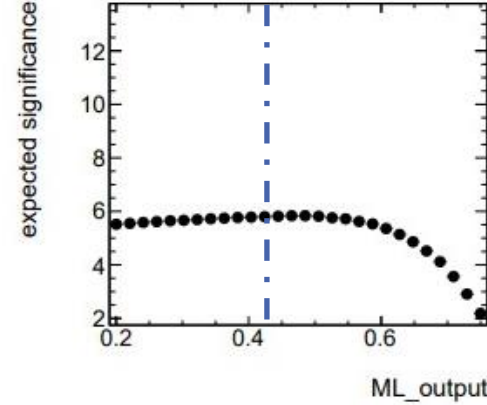
Table 5: Working point in different  $p_T^{\Xi_c^0}$  bin.



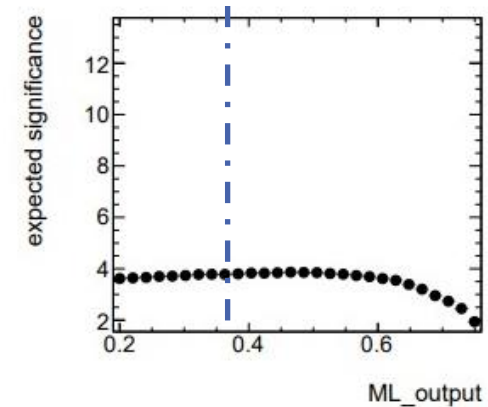
$2 < p_T < 4$  GeV/c



$4 < p_T < 6$  GeV/c



$6 < p_T < 8$  GeV/c



$8 < p_T < 12$  GeV/c

Keep enough statistics for low-mult

# ITS-TPC matching efficiency

ITS has only been used for  $\pi \leftarrow \Xi_c^0$

Only need to propagate the ITS-TPC matching efficiency of  $\pi$  to  $\Xi_c^0$

Systematics evaluated as:

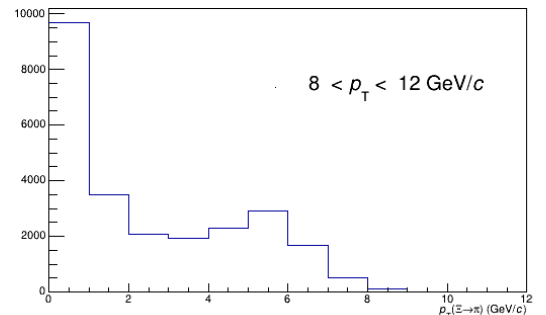
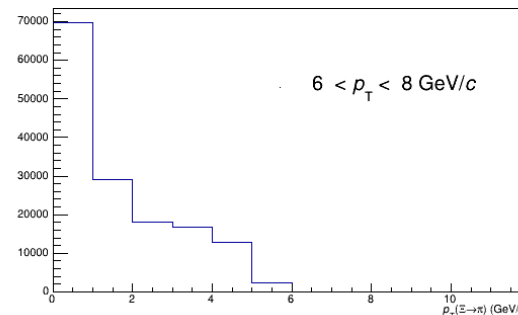
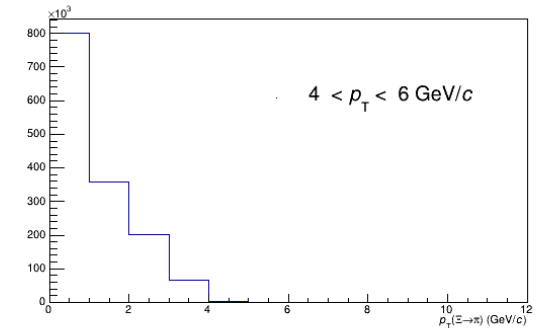
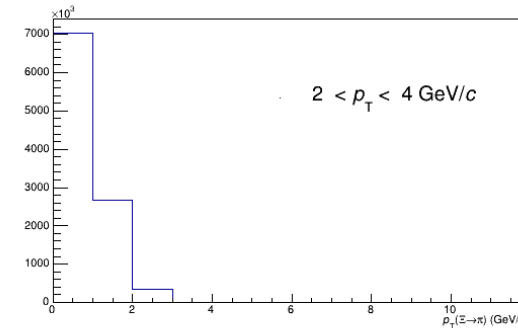
$$\text{Syst}_{\text{ITS-TPC matching}}^{\Xi_c^0} = \frac{\sum_{i=1}^N (\text{Syst}_i^{\pi \leftarrow \Xi_c^0} * \text{BC}_i)}{\sum_{i=1}^N \text{BC}_i}$$

- $\text{Syst}_i^{\pi \leftarrow \Xi_c^0}$  is the systematic of ITS-TPC matching in  $i^{\text{th}}$   $p_T^{\pi \leftarrow \Xi_c^0}$  bin

$p_T^{\pi \leftarrow \Xi_c^0}$ (GeV/c)	(0.5, 1.0)	(1, 2)	(2, 3)	(3, 4)	(4, 5)	(5, 6)	(6, 7)	(7, 8)	(8, 9)
ITS-TPC matching	1.1%	1.8%	2.7%	2.7%	2.3%	2.3%	2.4%	2.4%	3%

**Table 9:** The systematic uncertainties of ITS-TPC matching efficiency of  $\pi \leftarrow \Xi_c^0$  from DPG in each  $p_T$  bin.

- $\sum_{i=1}^N \text{BC}_i$  is the  $i^{\text{th}}$  bin content in  $p_T^{\pi \leftarrow \Xi_c^0}$  distribution for each bin  $p_T^{\Xi_c^0}$

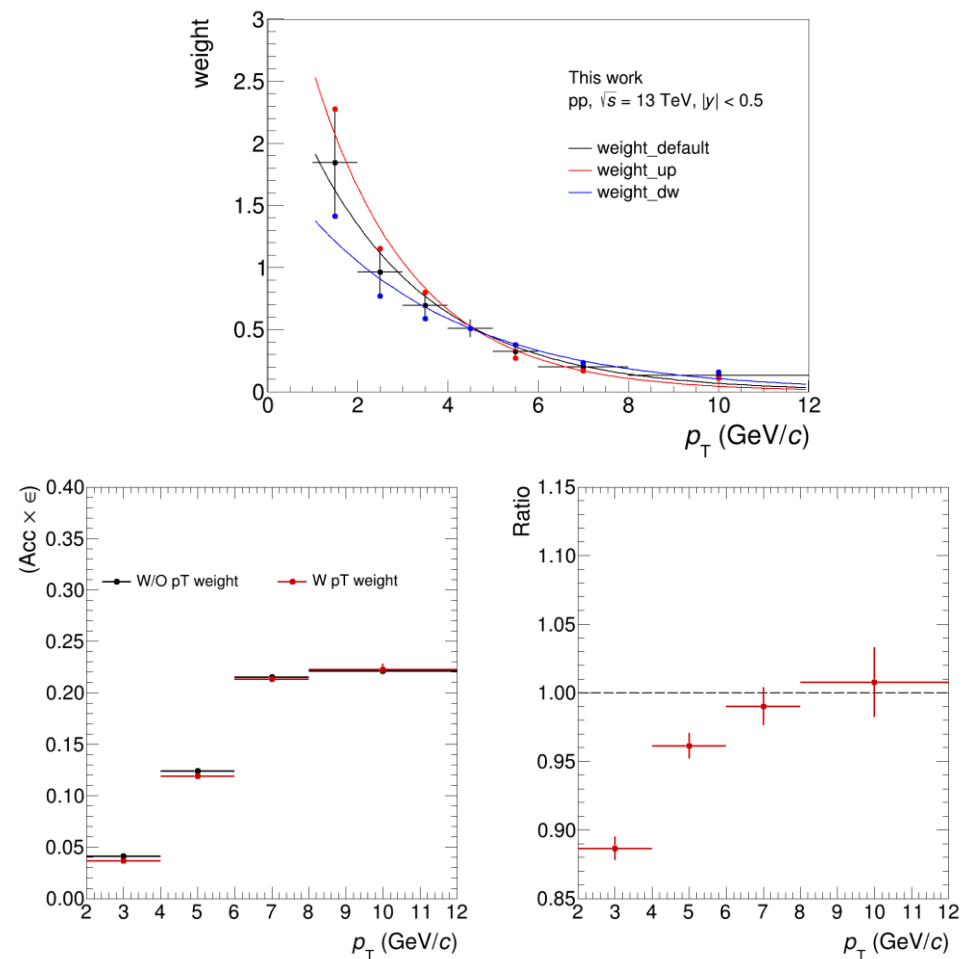


$p_T^{\Xi_c^0}$ (GeV/c)	(2, 4)	(4, 6)	(6, 8)	(8, 12)
ITS-TPC matching	1%	2%	2%	2%

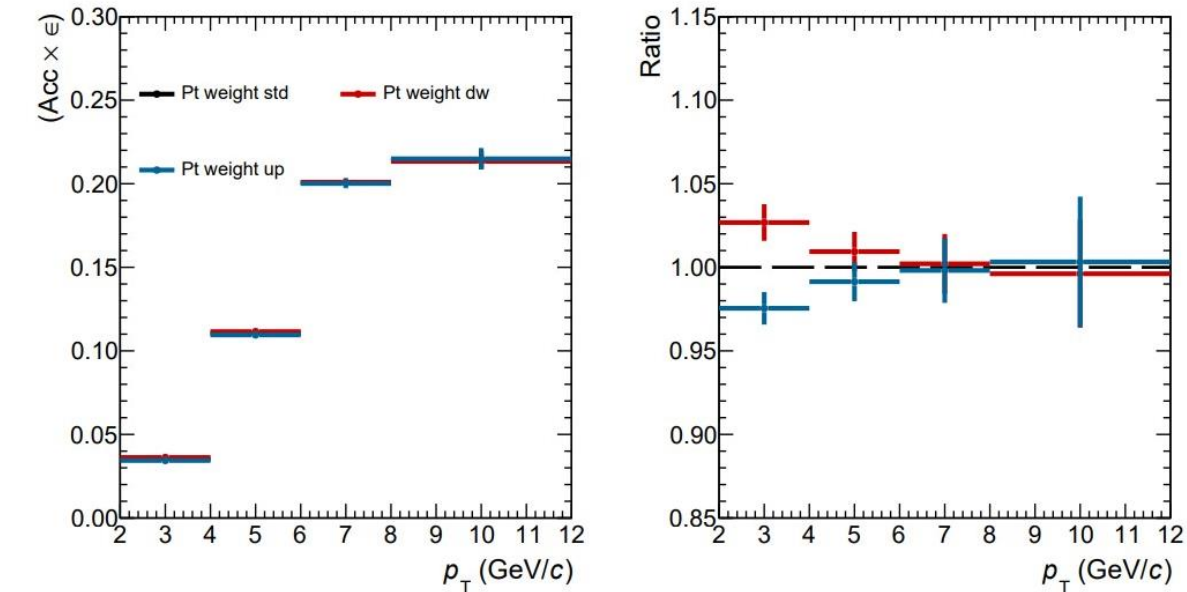
The systematic uncertainties of ITS-TPC matching efficiency for  $\Xi_c^0$  in each  $p_T$  bin.

# $p_T$ weight

The weights are computed dividing the  $p_T$  shape obtained from data and obtained from PYTHIA 8



Eff W and W/O  $p_T$  central-weight



Comparison between the efficiencies obtained by re-weighting the  $p_T$  shape

Systematics evaluated at: *RMS*

$p_T^{\Xi_c^0}$ (GeV/c)	(2, 4)	(4, 6)	(6, 8)	(8, 12)
MC $p_T$ shape	3.0%	1.0%	0.%	0%

$\tau_{th}$  The systematic uncertainties of MC  $p_T$  shape for  $\Xi_c^0$  in each  $p_T$  bin.

# Multiplicity dependence of feed-down

The dependence of B hadrons on the charged particle density may vary

## Single spectra:

Consider the upper and lower values of the uncertainties on  $f_{\text{prompt}}$  and the same parameter considered in the multiplicity-integrated and multiplicity bins.

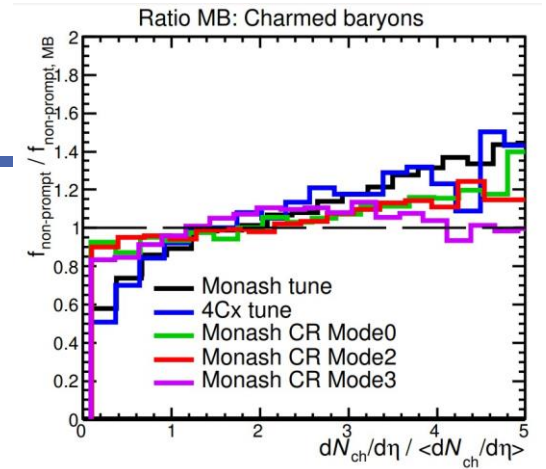
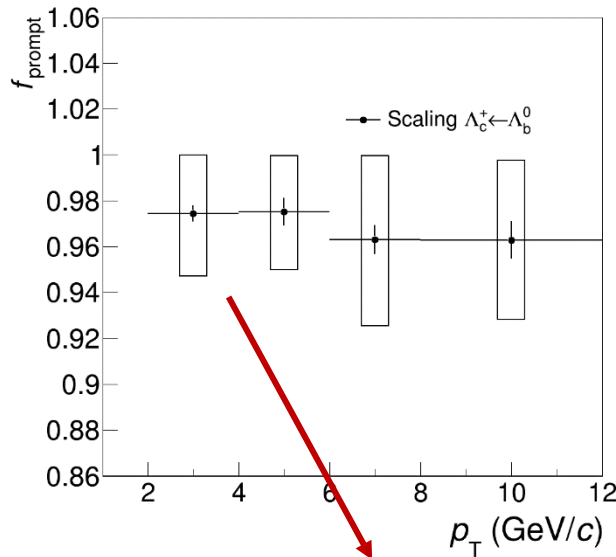
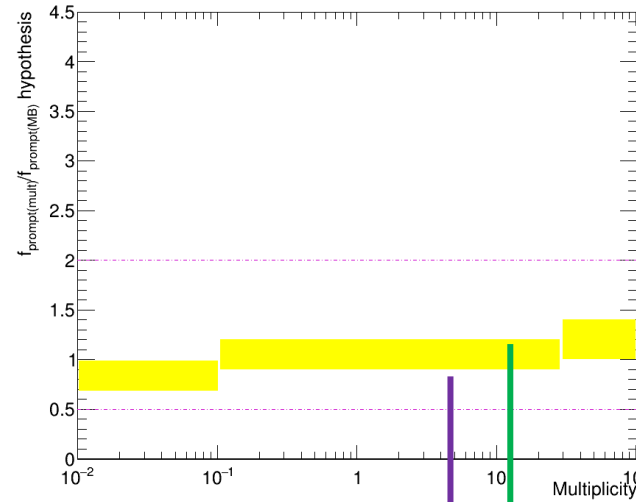


figure come from  $\Lambda_c$

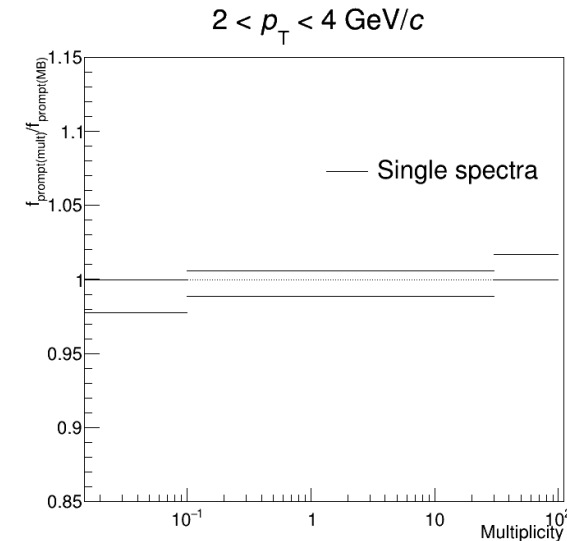


$$f_B(\text{MB}) = 1 - f_{\text{prompt}}(\text{MB})$$



$$f_B^{\text{Min}}(\text{mult}) = f_B(\text{MB}) * r^{\text{MIN}}(\text{mult})$$

$$f_B^{\text{Max}}(\text{mult}) = f_B(\text{MB}) * r^{\text{MAX}}(\text{mult})$$



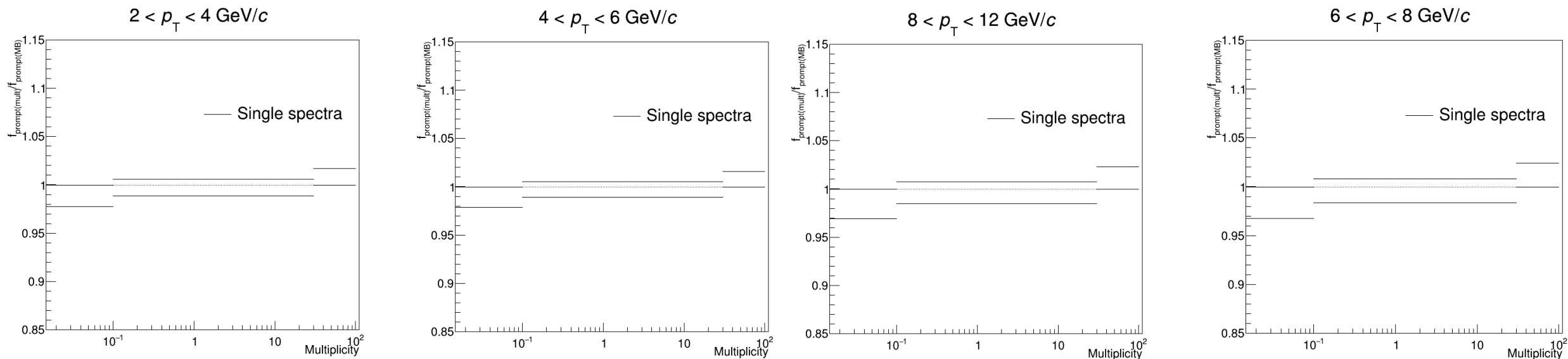
Same structure as  $\Lambda_c$

$$f_{\text{prompt}}^{\text{Max}}(\text{mult}) = 1 - f_B^{\text{Min}}(\text{mult})$$

$$f_{\text{prompt}}^{\text{Min}}(\text{mult}) = 1 - f_B^{\text{Max}}(\text{mult})$$



# Multiplicity dependence of feed-down



Multiplicity interval	$f_{non-prompt}$ variation
30-100 $VOM_{perc}$	[0.7 - 1.0]
0.1-30 $VOM_{perc}$	[0.9 - 1.2]
0-0.1 $VOM_{perc}$	[1.0 - 1.4]

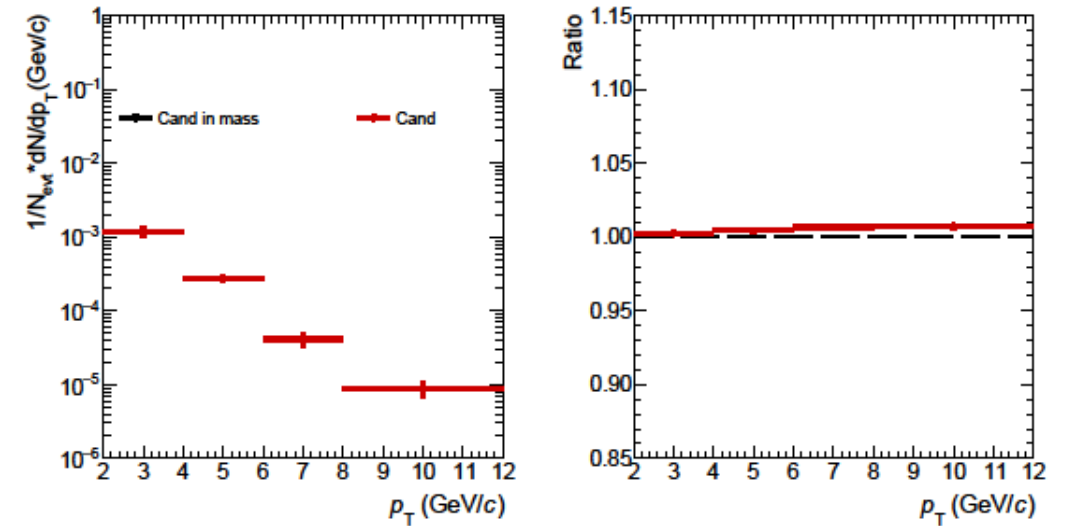
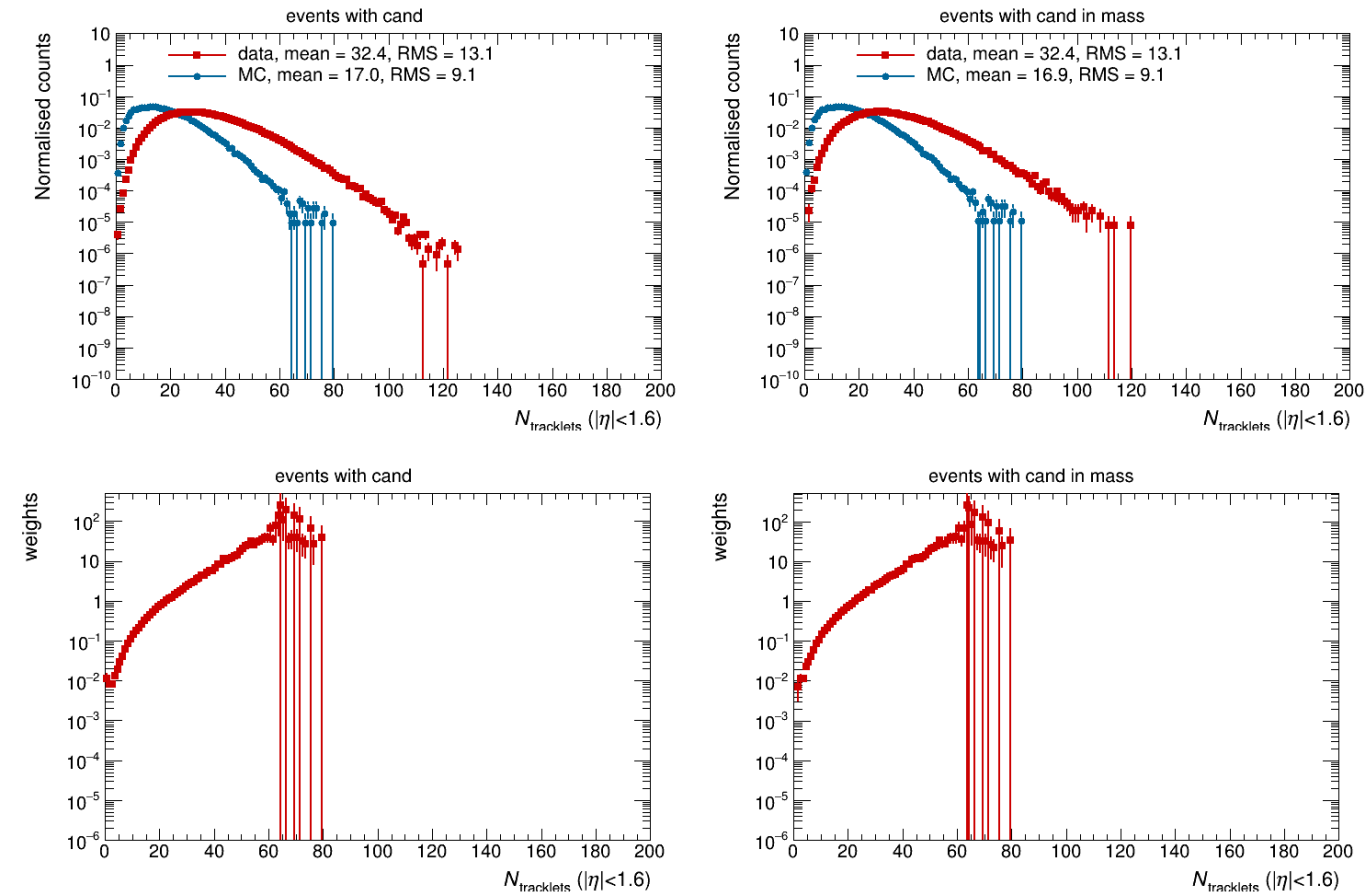
**Table 13:** Variations on fnon-prompt used for the different multiplicity bins.

$p_T^{\Xi_c^0}$ (GeV/c)		(2, 4)	(4, 6)	(6, 8)	(8, 12)
30-100	up	1.7%	1.6%	2.4%	-
	dw	0.0%	0.0%	0.0%	-
0.1-30	up	0.6%	0.5%	0.8%	0.7%
	dw	1.2%	1.1%	1.7%	2.5%
0-0.1	up	0.0%	0.0%	0.0%	0.0%
	dw	2.2%	2.2%	2.4%	3.1%

Systematic uncertainties due to the multiplicity dependence in the feed-down subtraction for  $X_{ic}$ .

# Mult.-weight

Ntrkl distribution of the events in the 0.1%-30% multiplicity with at least a  $\Xi_c^0$  candidate (left) and events with at least a  $\Xi_c^0$  candidate in mass range of PDG mass  $\pm 2\sigma$  MeV (right) [2.452, 2.488]. Bottom is ratio of the data with respect to MC for two cases.



Systematics evaluated at: *Shift*  
Assigned systematics to 0-1%

# Raw yield extraction

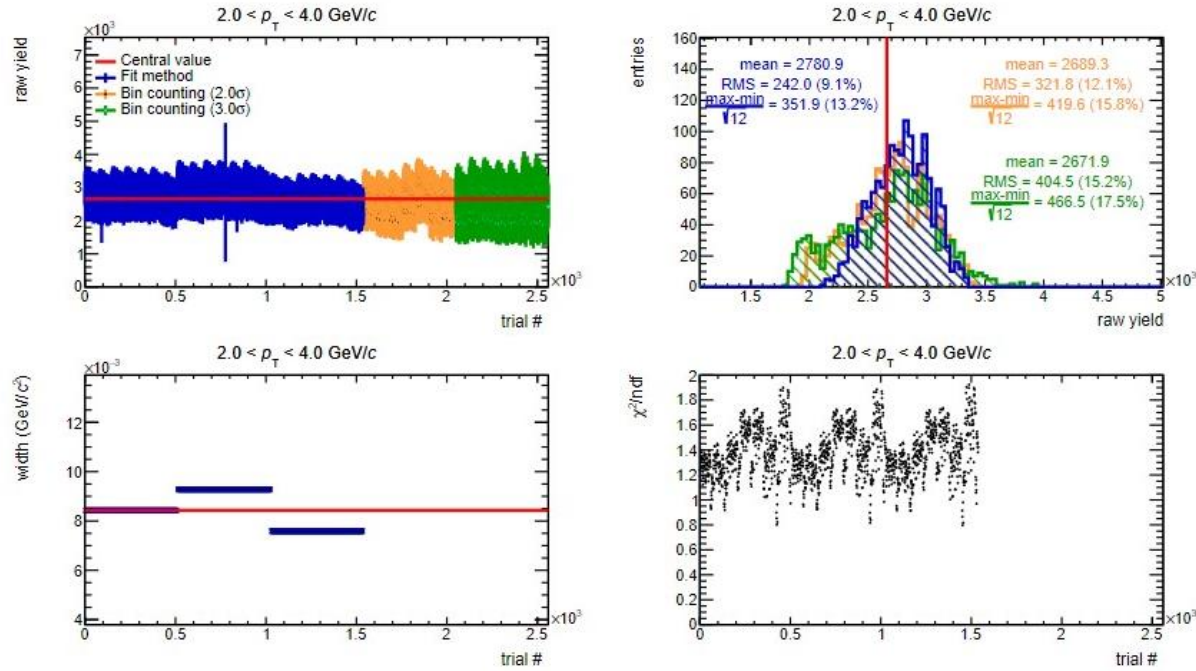


**Fig. 30:** Raw yield systematic for  $p_T$  bin 2 GeV/c-4 GeV/c and [0,0.1]V0M percentile multiplicity

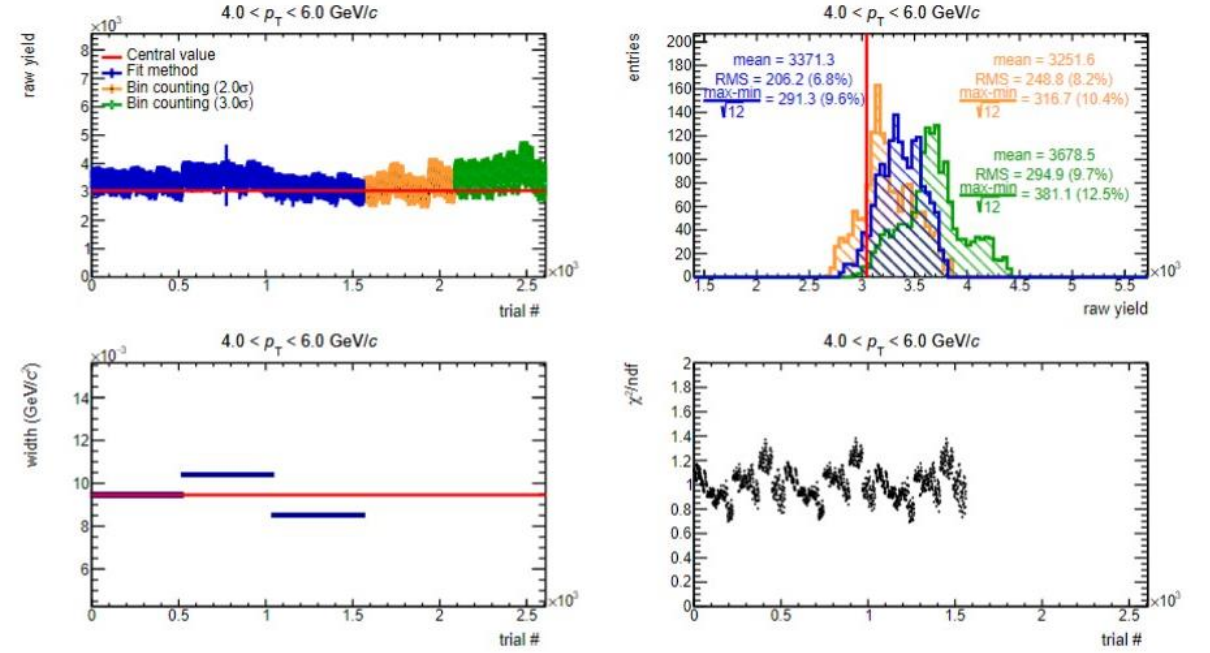


**Fig. 28:** Raw yield systematic for  $p_T$  bin 4 GeV/c-6 GeV/c and [0,0.1]V0M percentile multiplicity

# Raw yield extraction

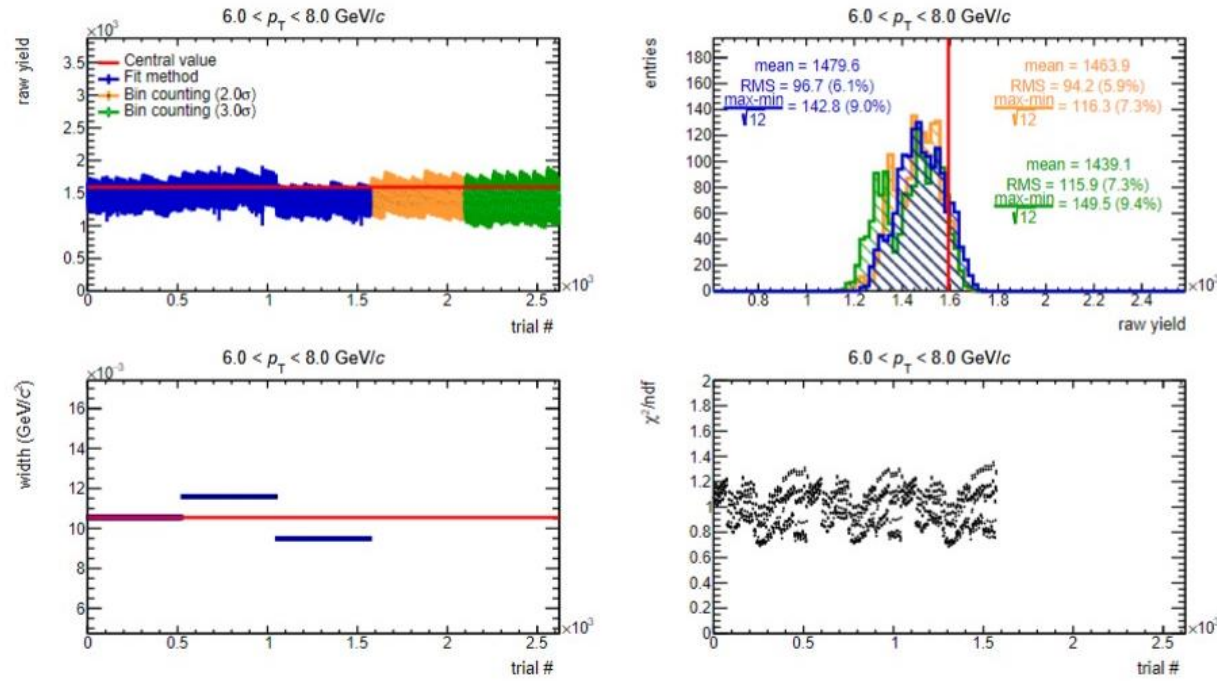


Fig. 29: Raw yield systematic for  $p_T$  bin 6GeV/c-8GeV/c and  $[0,0.1]$ V0M percentile multiplicity

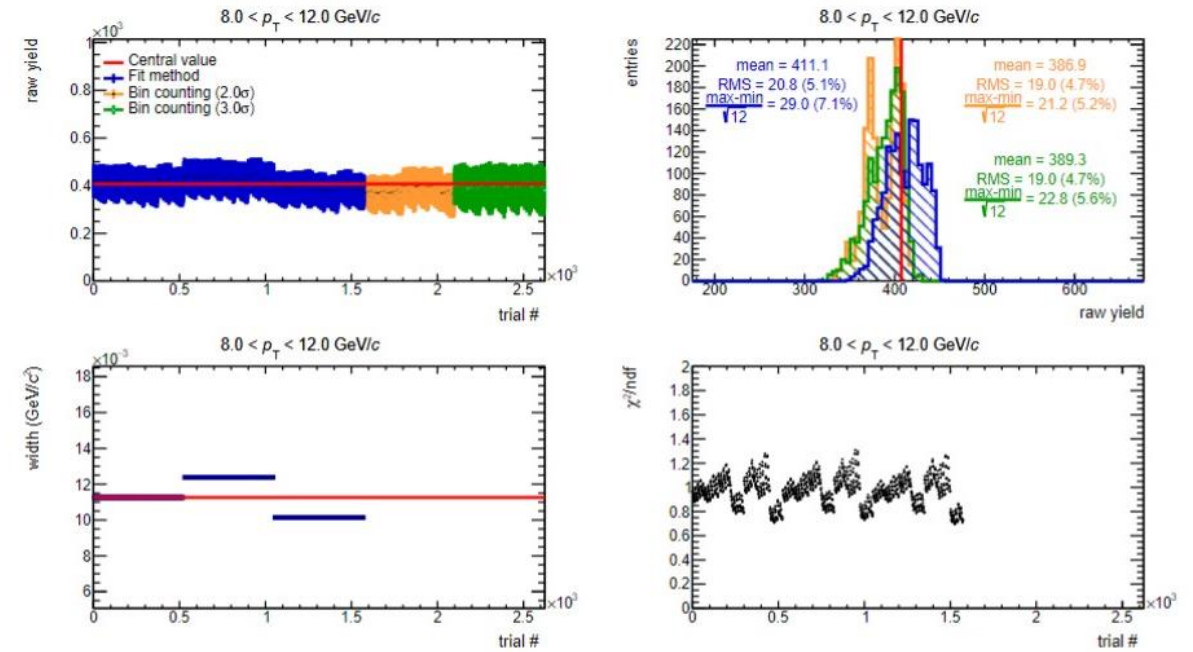
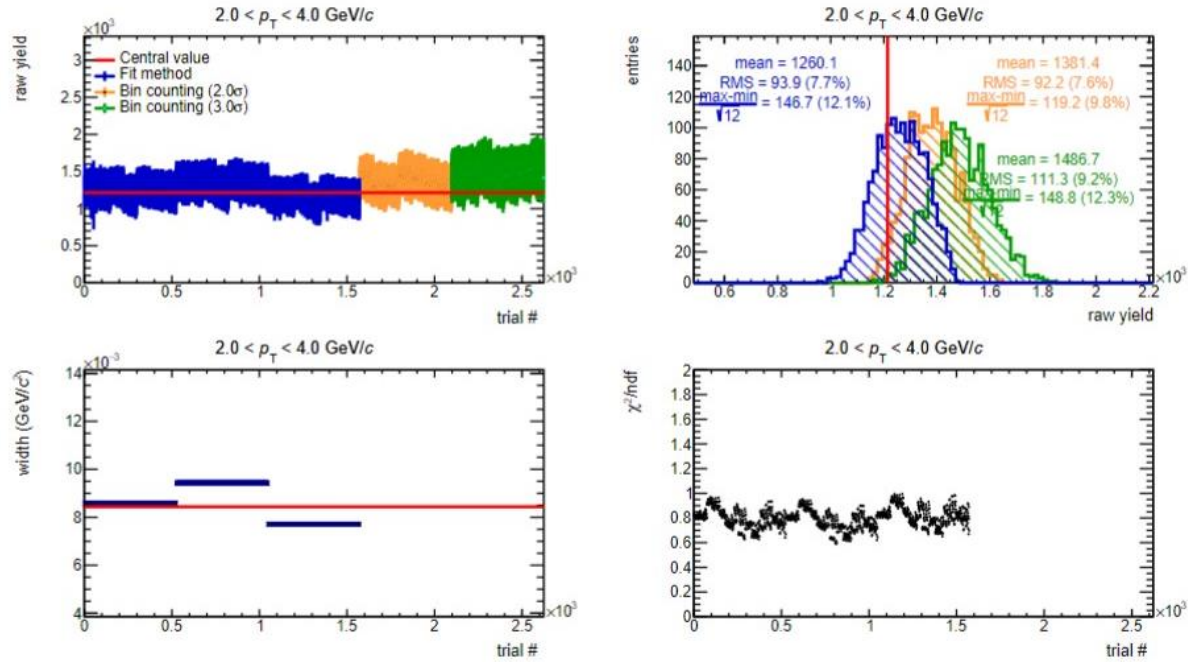


Fig. 30: Raw yield systematic for  $p_T$  bin 8GeV/c-12GeV/c and  $[0,0.1]$ V0M percentile multiplicity



# Raw yield extraction



**Fig. 31:** Raw yield systematic for  $p_T$  bin 2GeV/c-4GeV/c and [0.1,30]V0M percentile multiplicity

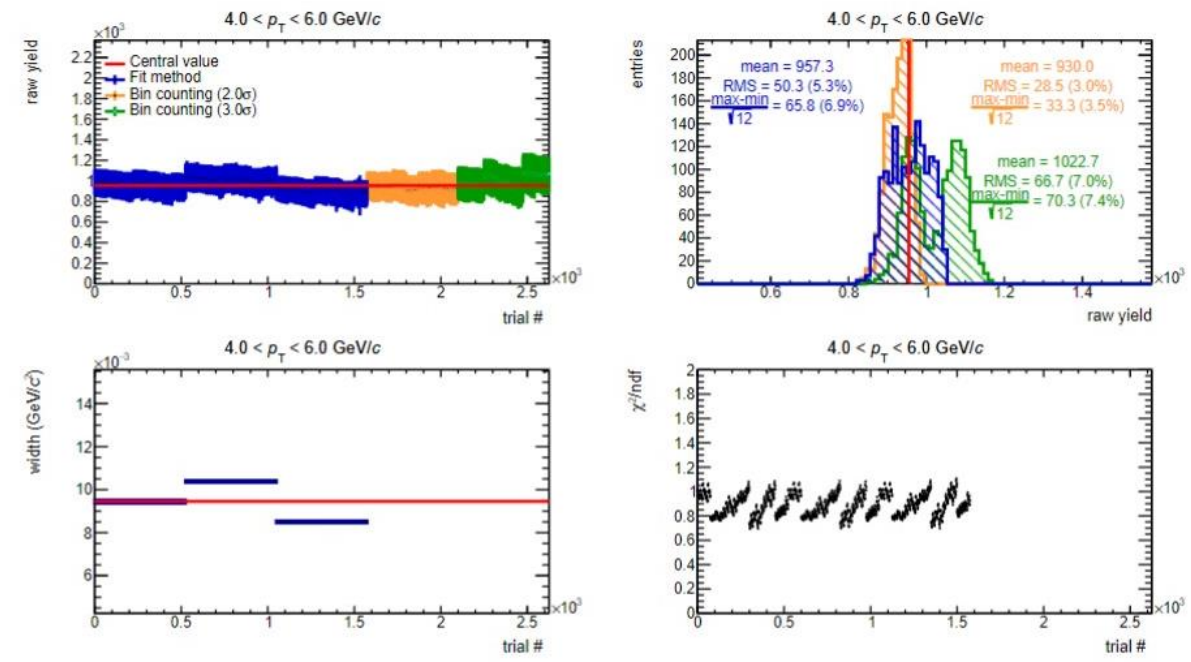


**Fig. 32:** Raw yield systematic for  $p_T$  bin 4GeV/c-6GeV/c and [0.1,30]V0M percentile multiplicity

# Raw yield extraction

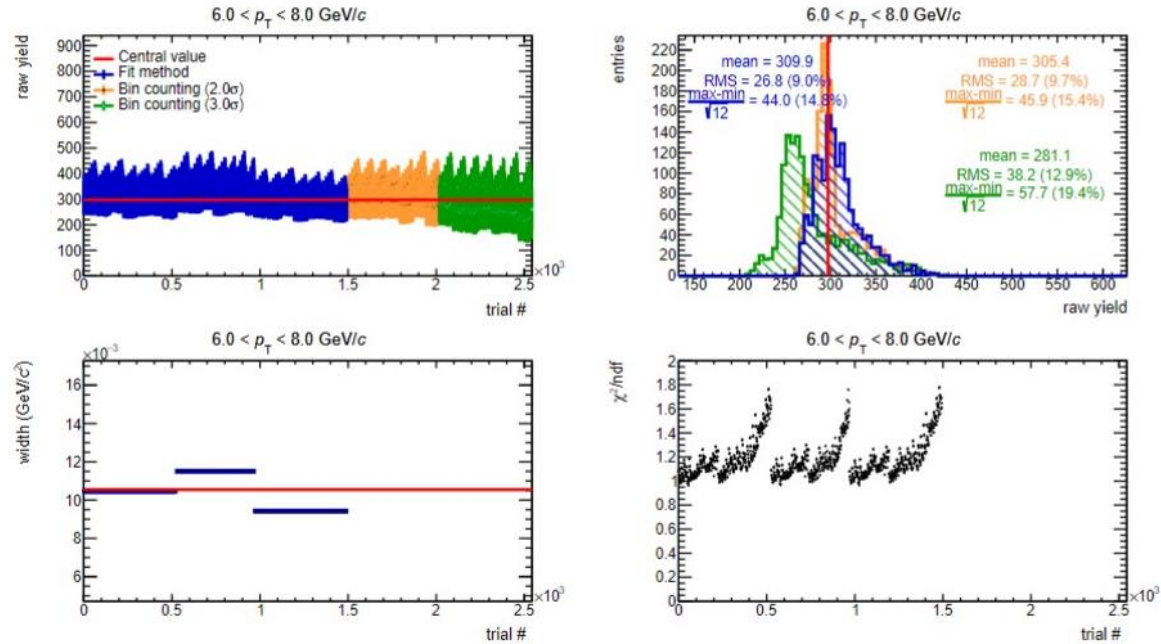


Fig. 33: Raw yield systematic for  $p_T$  bin 6GeV/c-8GeV/c and [0.1,30]V0M percentile multiplicity

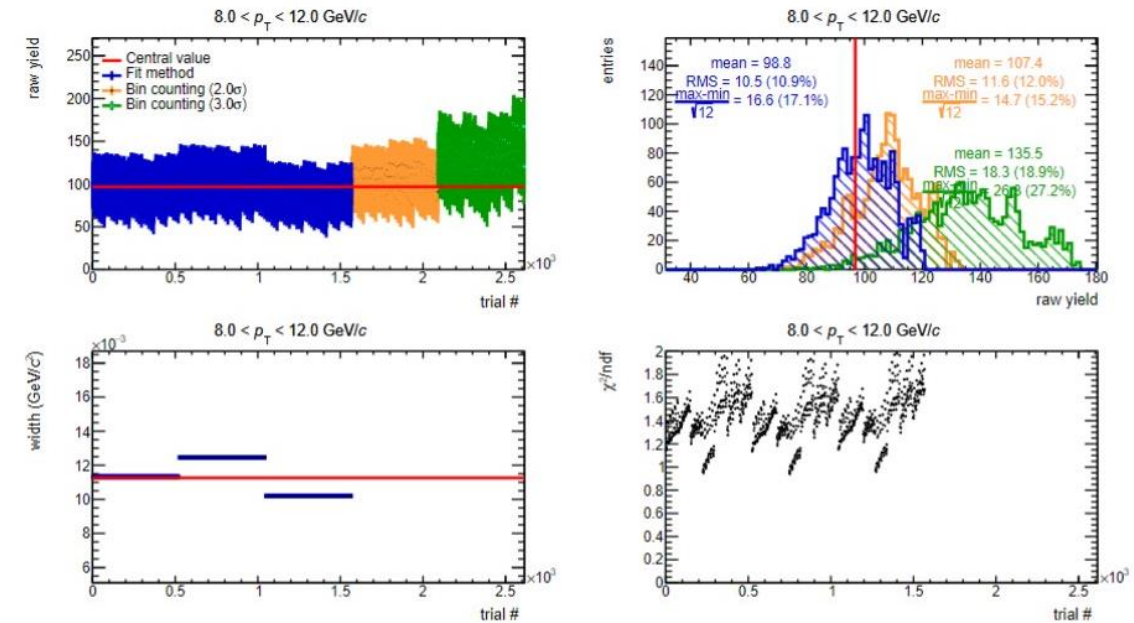


Fig. 34: Raw yield systematic for  $p_T$  bin 8GeV/c-12GeV/c and [0.1,30]V0M percentile multiplicity

# Raw yield extraction

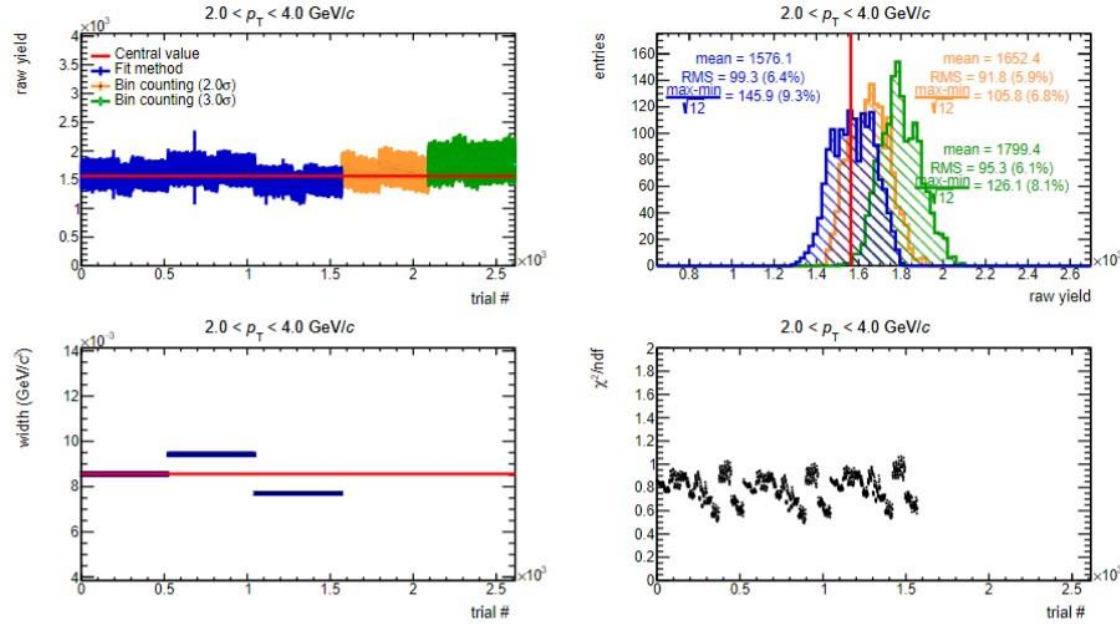


Fig. 35: Raw yield systematic for  $p_T$  bin 2GeV/c-4GeV/c and integrated V0M percentile multiplicity

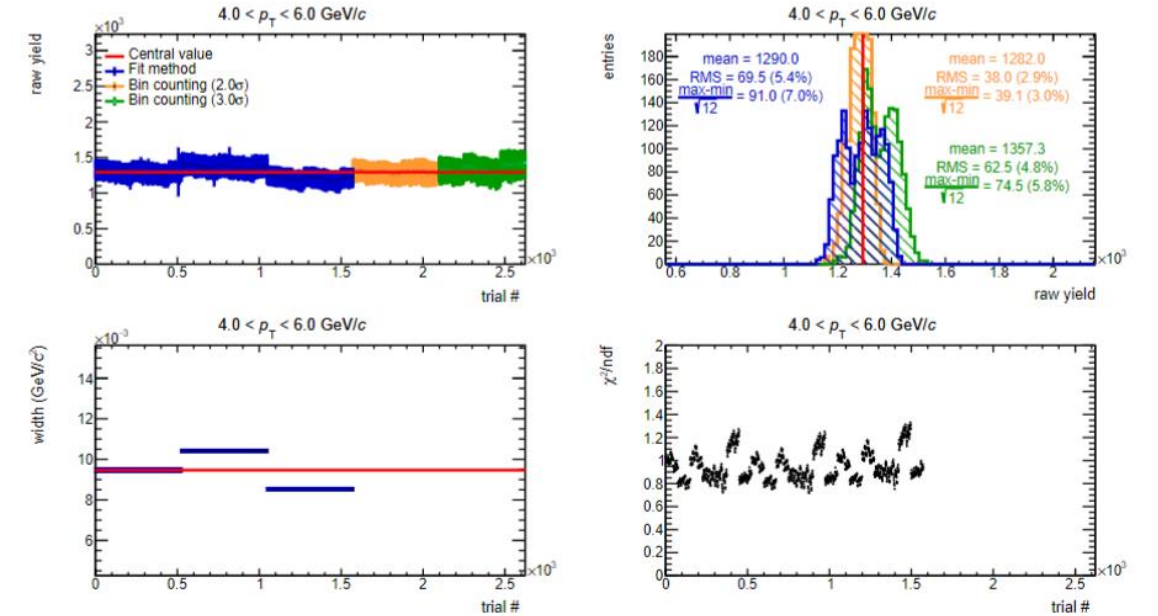


Fig. 36: Raw yield systematic for  $p_T$  bin 4GeV/c-6GeV/c and integrated V0M percentile multiplicity

# Raw yield extraction

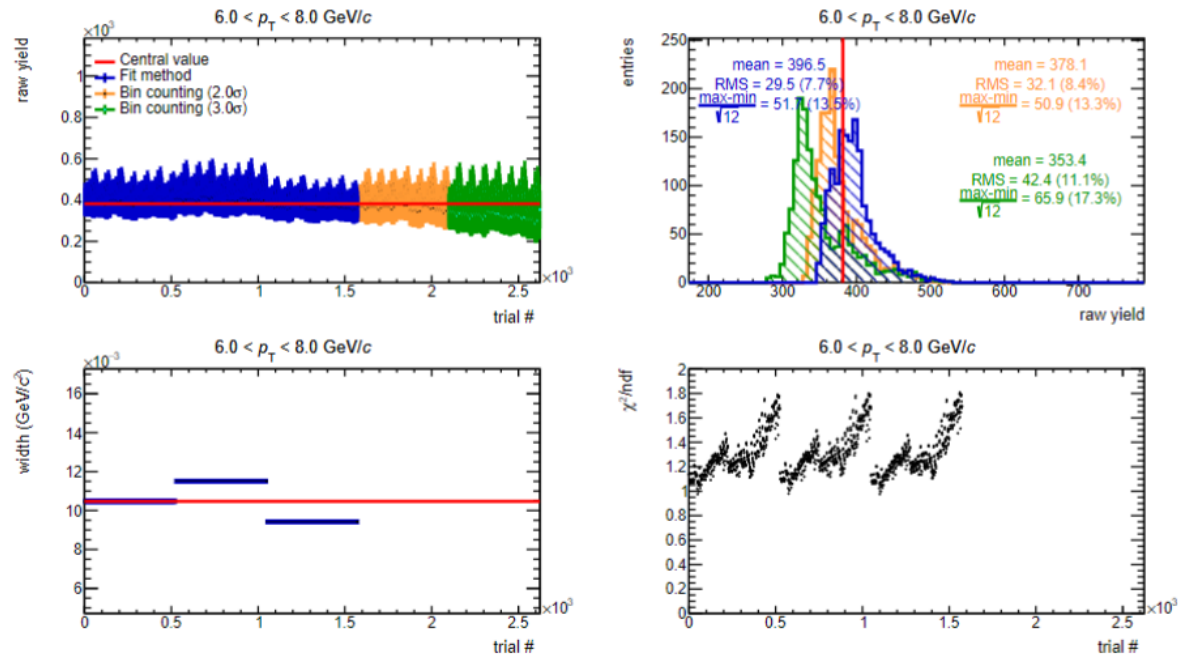


Fig. 37: Raw yield systematic for  $p_T$  bin 6GeV/c-8GeV/c and integrated V0M percentile multiplicity

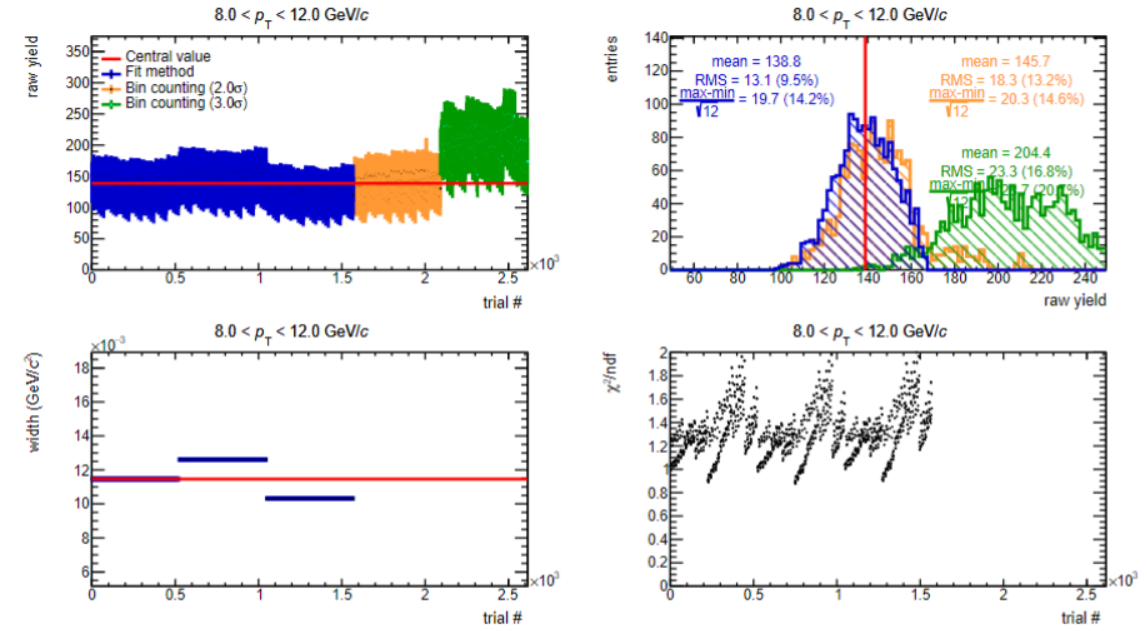


Fig. 38: Raw yield systematic for  $p_T$  bin 8GeV/c-12GeV/c and integrated V0M percentile multiplicity



# Raw yield extraction

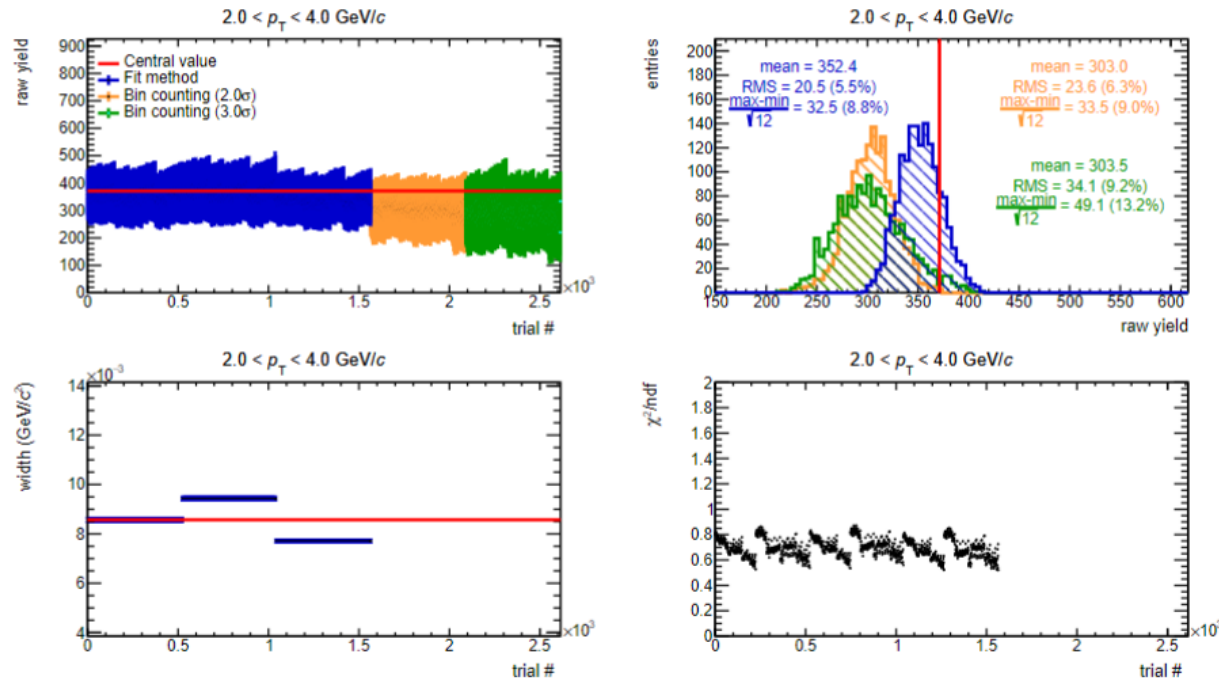


Fig. 39: Raw yield systematic for  $p_T$  bin 2GeV/c-4GeV/c and [30,100]V0M percentile multiplicity

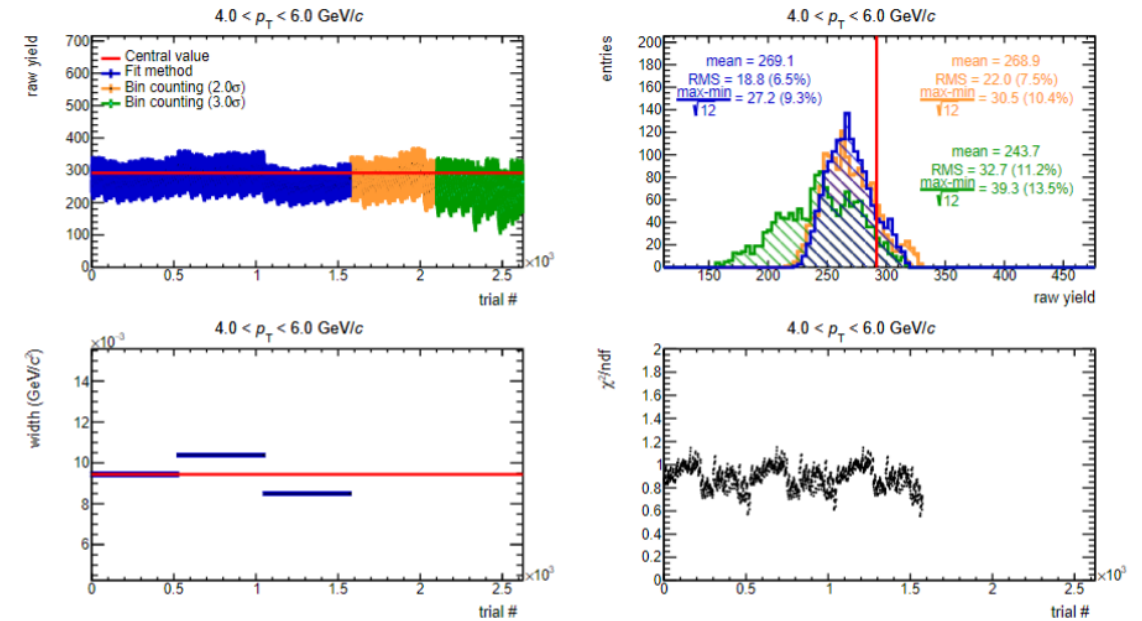
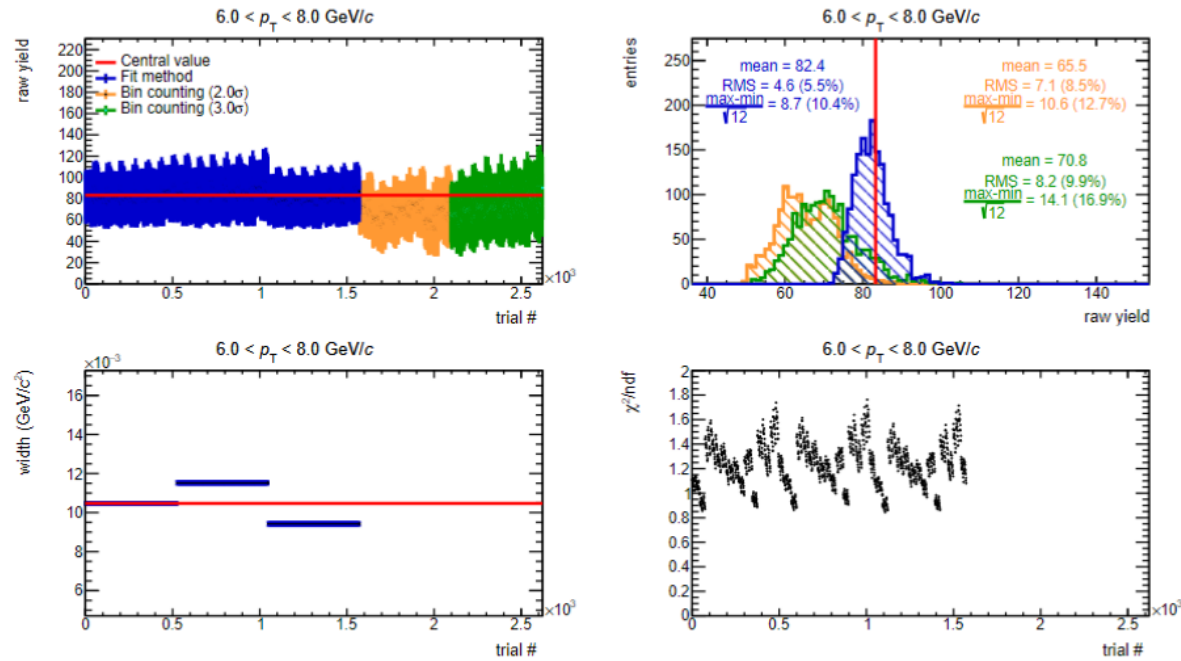


Fig. 40: Raw yield systematic for  $p_T$  bin 4GeV/c-6GeV/c and [30,100]V0M percentile multiplicity

# Raw yield extraction



**Fig. 41:** Raw yield systematic for  $p_T$  bin 6GeV/c-8GeV/c and [30,100]V0M percentile multiplicity

# BDT

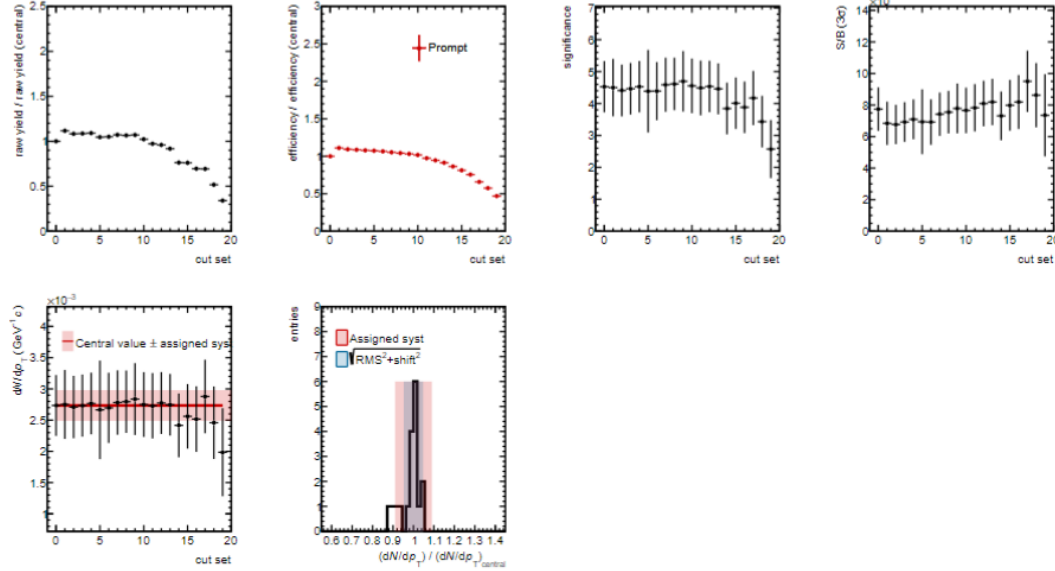


Fig. 42: The cut-variation studies for  $p_T$  bin 2 GeV/c-4 GeV/c and [0,0.1]V0M percentile multiplicity

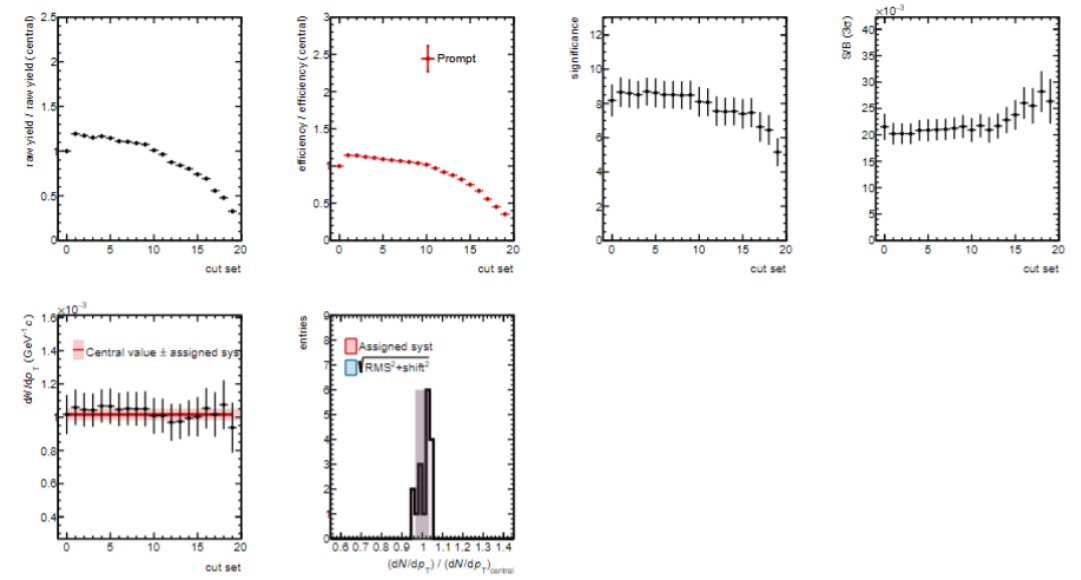
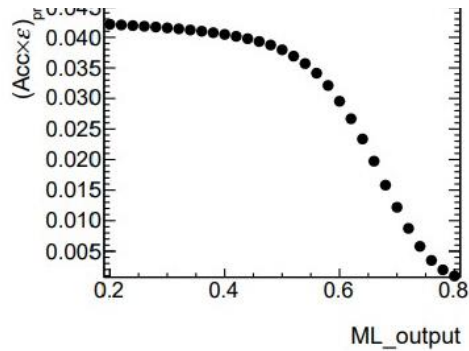
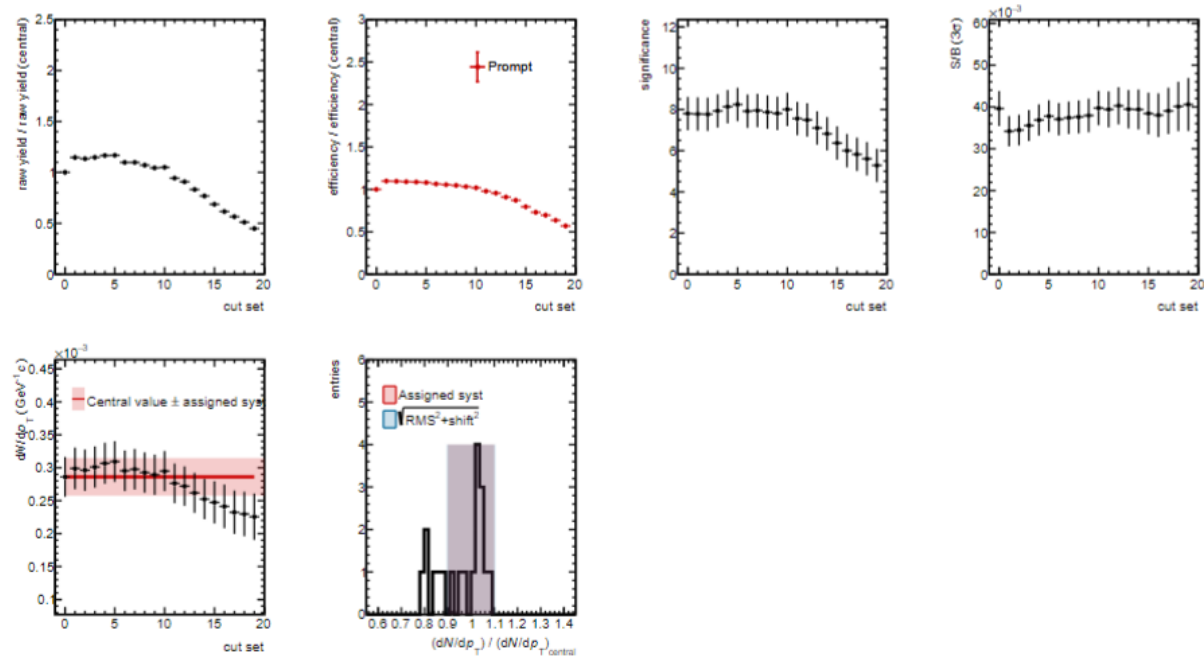


Fig. 43: The cut-variation studies for  $p_T$  bin 4 GeV/c-6 GeV/c and [0,0.1]V0M percentile multiplicity



Eff at 2-4 GeV/c

# BDT



**Fig. 44:** The cut-variation studies for  $p_T$  bin 6 GeV/c-8 GeV/c and [0,0.1]V0M percentile multiplicity

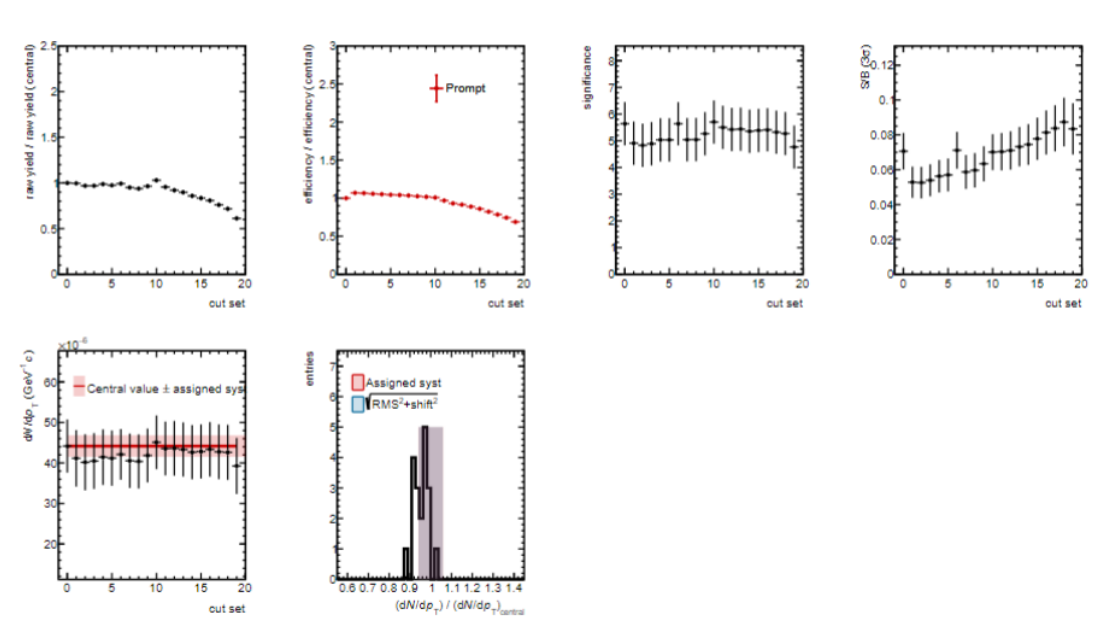


**Fig. 45:** The cut-variation studies for  $p_T$  bin 8 GeV/c-12 GeV/c and [0,0.1]V0M percentile multiplicity

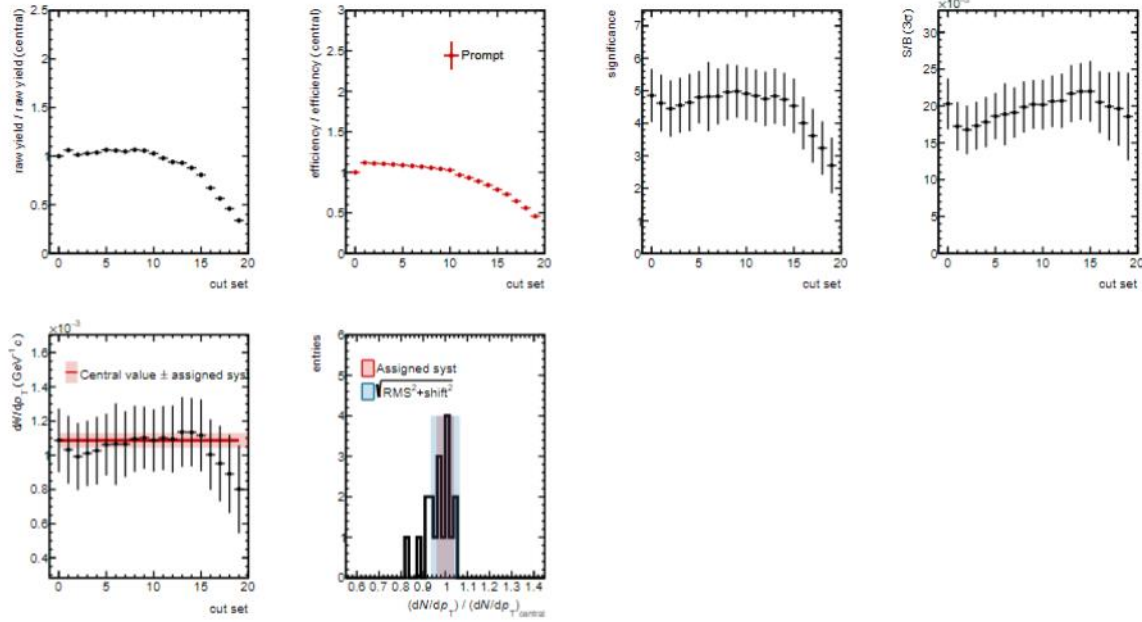


**Fig. 46:** The cut-variation studies for  $p_T$  bin 2 GeV/c-4 GeV/c and [0.1,30]V0M percentile multiplicity

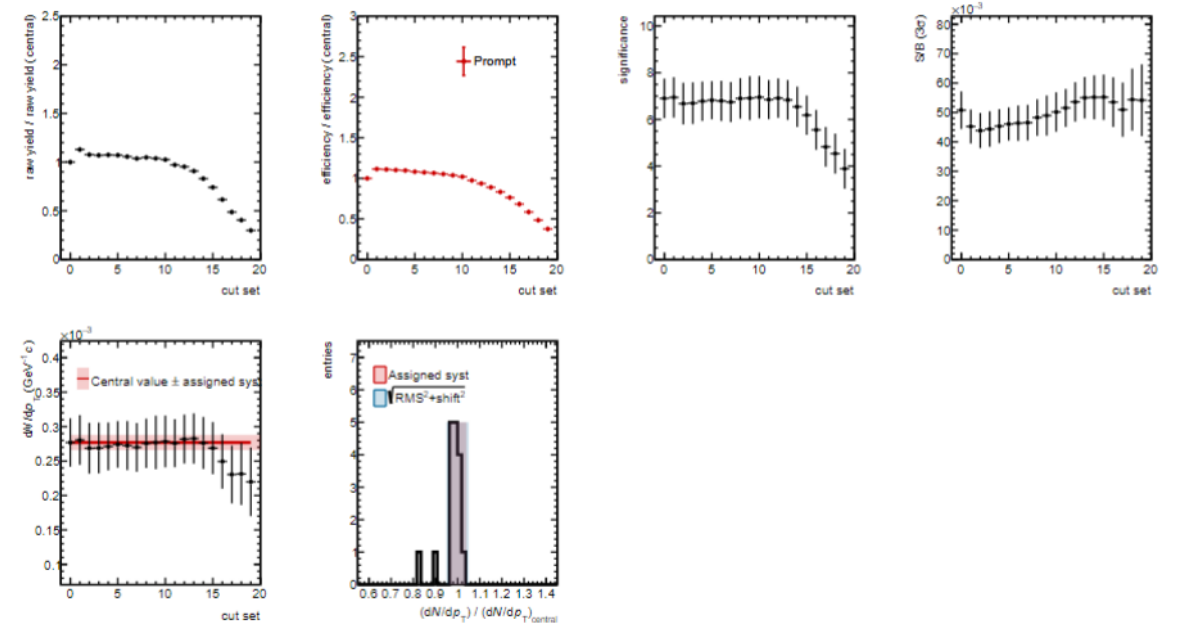


**Fig. 47:** The cut-variation studies for  $p_T$  bin 4 GeV/c-6 GeV/c and [0.1,30]V0M percentile multiplicity

# BDT

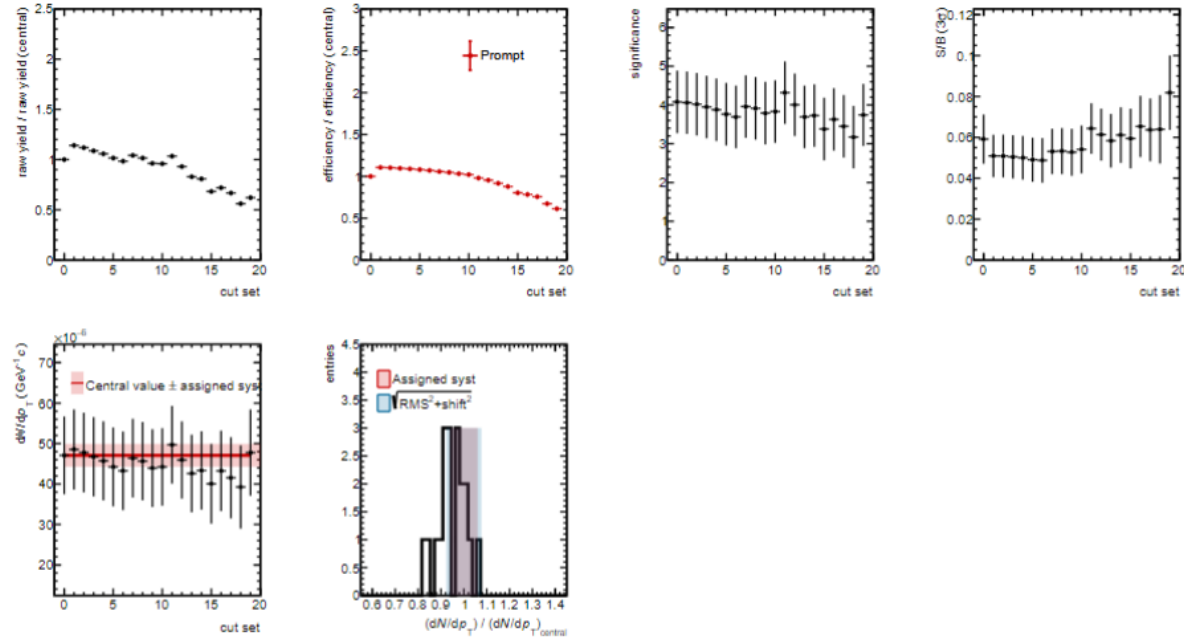


**Fig. 48:** The cut-variation studies for  $p_T$  bin 6 GeV/c-8 GeV/c and [0.1,30]V0M percentile multiplicity

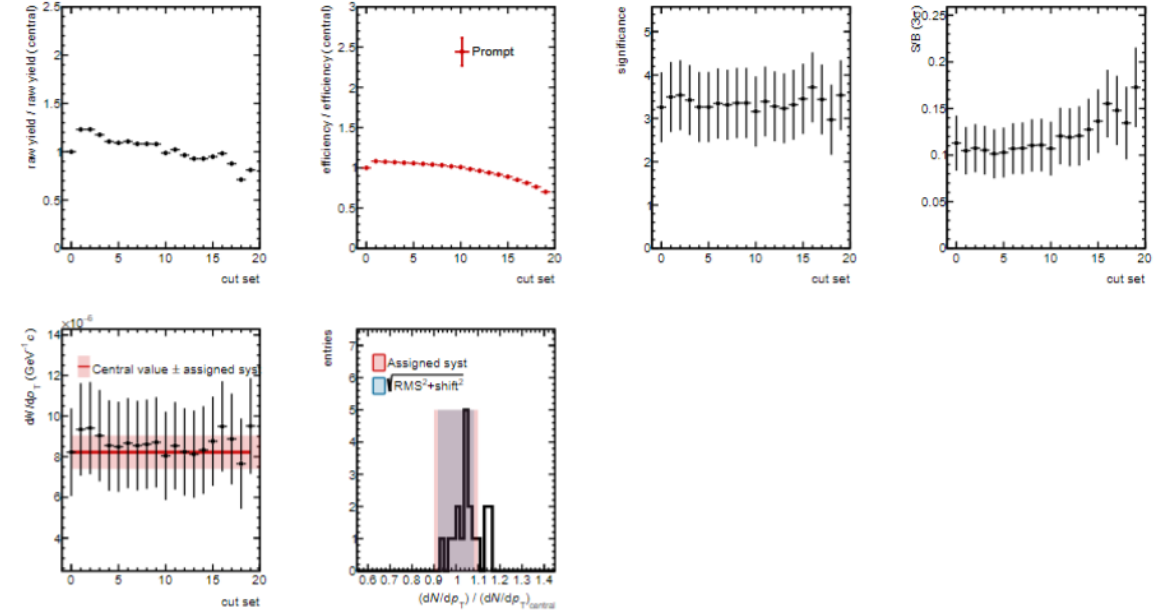


**Fig. 49:** The cut-variation studies for  $p_T$  bin 8 GeV/c-12 GeV/c and [0.1,30]V0M percentile multiplicity

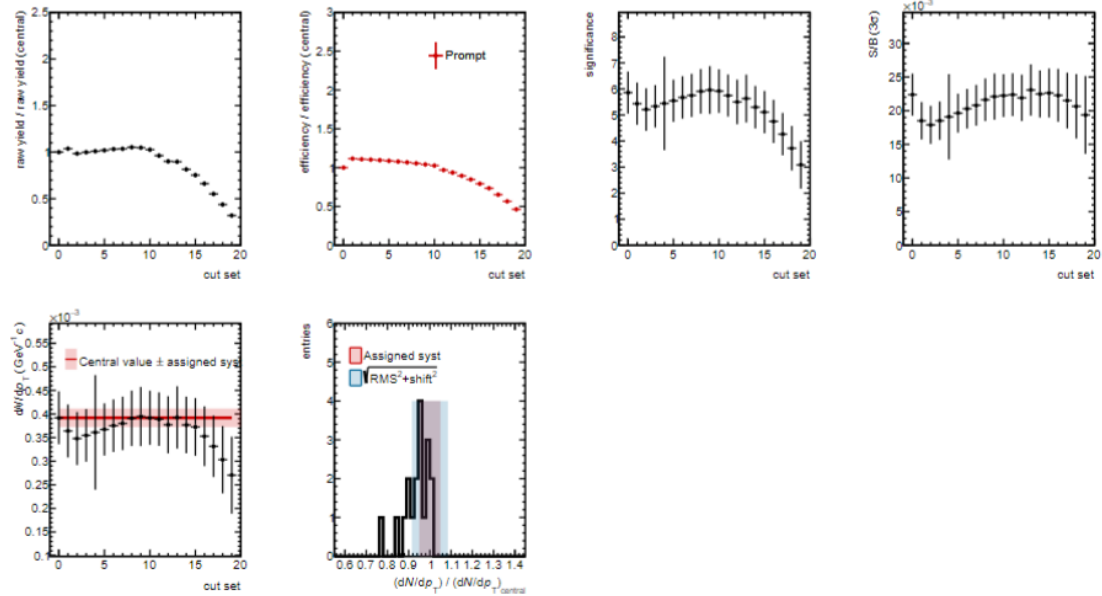


**Fig. 50:** The cut-variation studies for  $p_T$  bin 2GeV/c-4GeV/c and [0,100]V0M percentile multiplicity

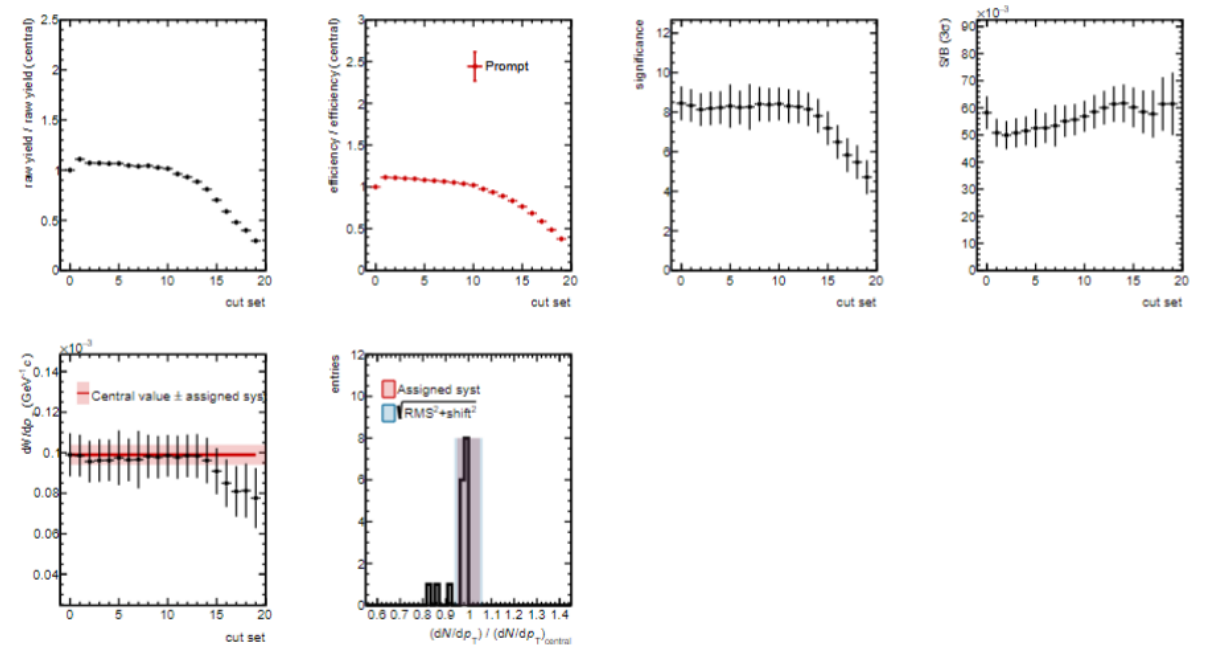


**Fig. 51:** The cut-variation studies for  $p_T$  bin 4GeV/c-6GeV/c and [0,100]V0M percentile multiplicity

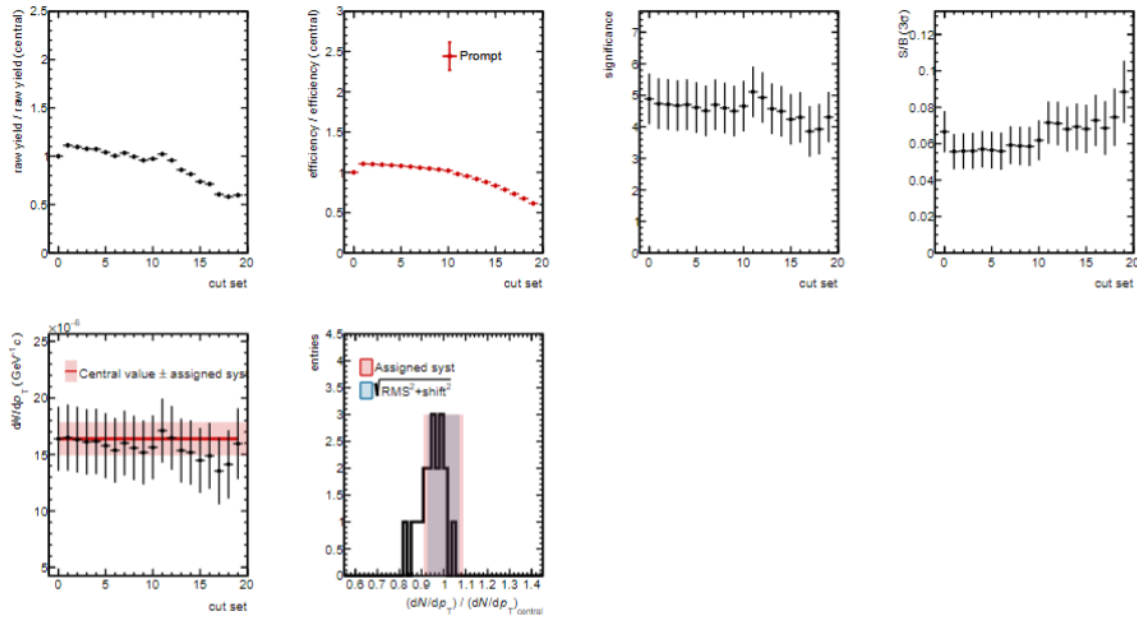


**Fig. 52:** The cut-variation studies for  $p_T$  bin 6GeV/c-8GeV/c and [0,100]V0M percentile multiplicity

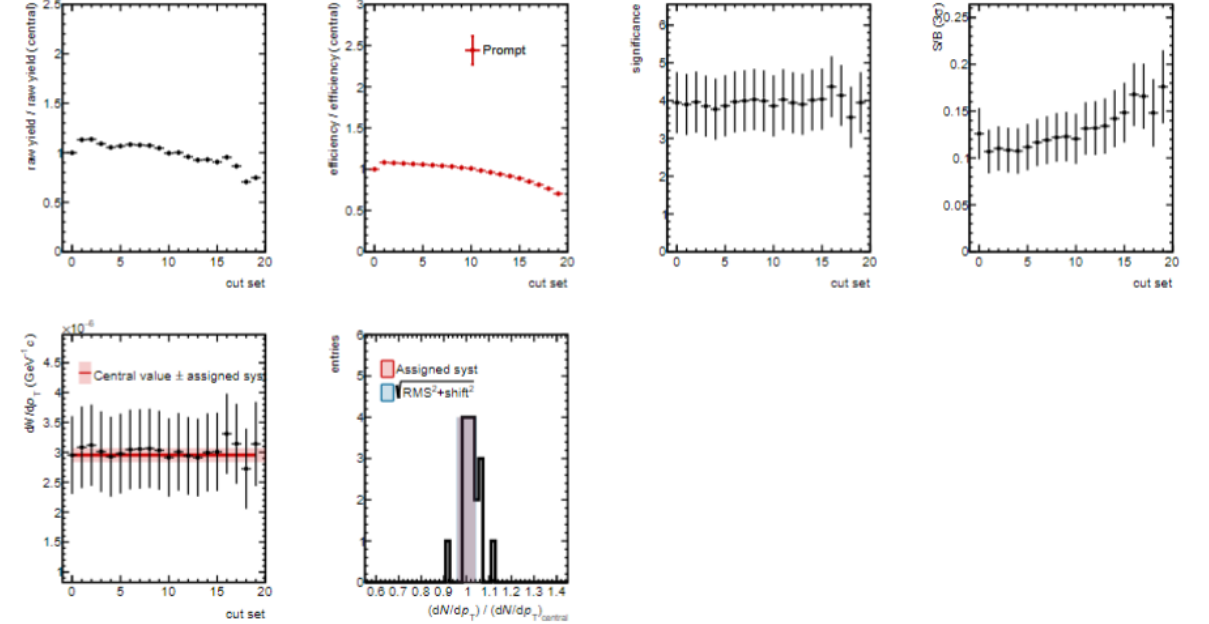


**Fig. 53:** The cut-variation studies for  $p_T$  bin 8GeV/c-12GeV/c and [0,100]V0M percentile multiplicity



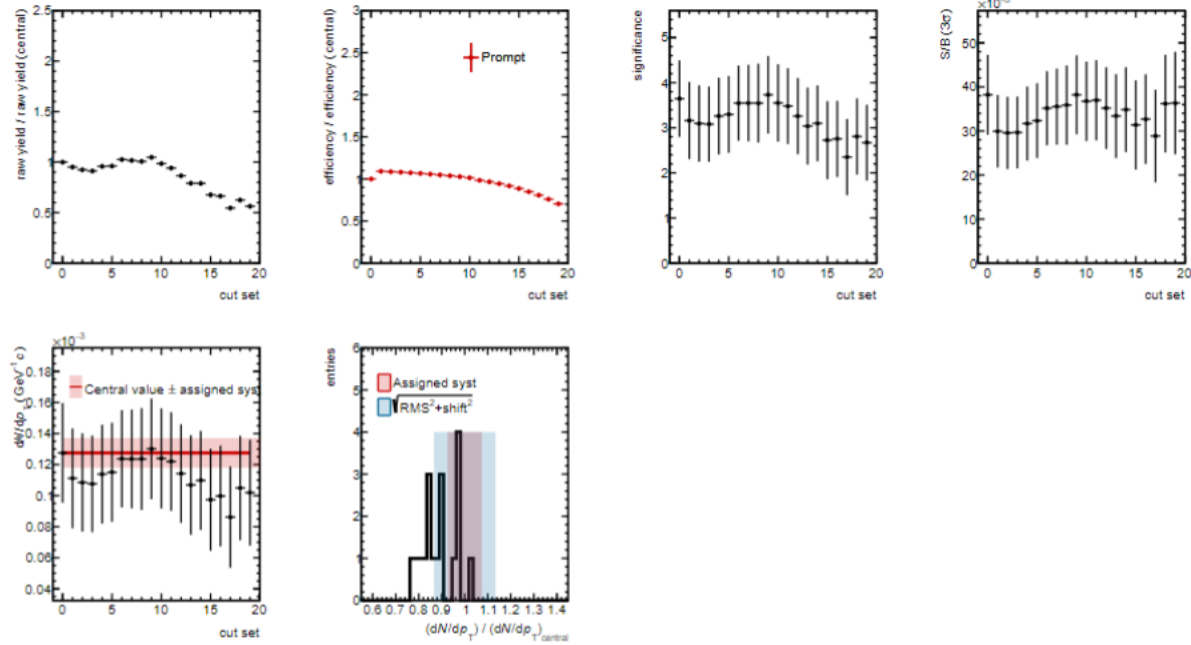


**Fig. 54:** The cut-variation studies for  $p_T$  bin 2GeV/c-4GeV/c and [30,100]V0M percentile multiplicity

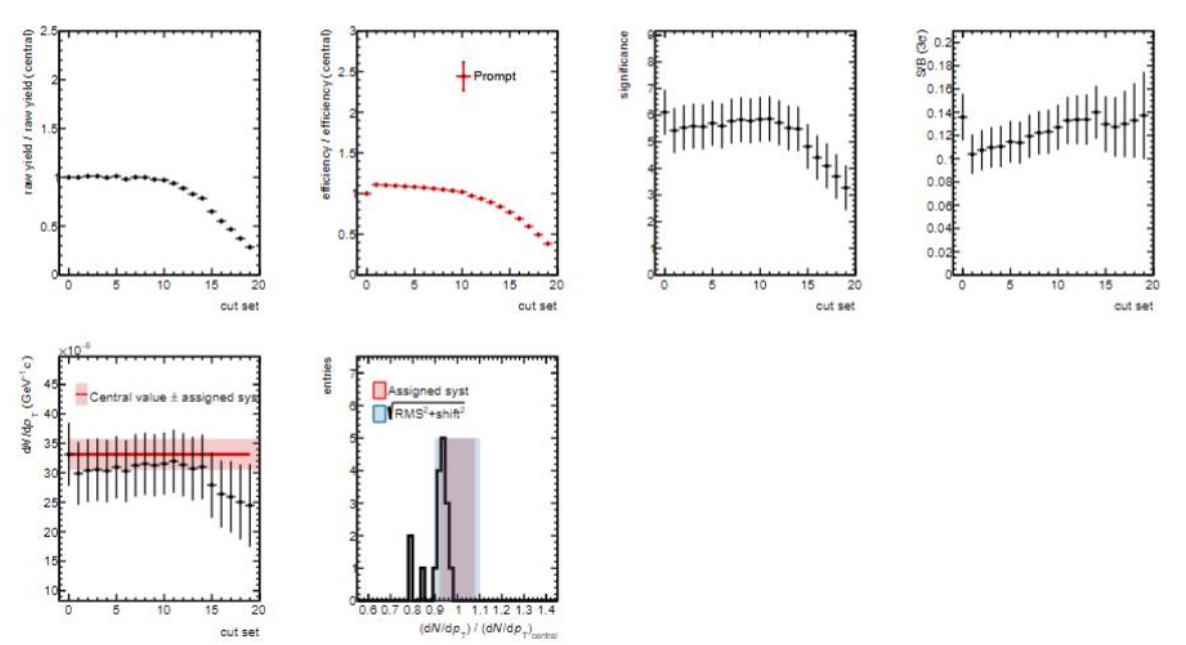


**Fig. 55:** The cut-variation studies for  $p_T$  bin 4GeV/c-6GeV/c and [30,100]V0M percentile multiplicity

# BDT

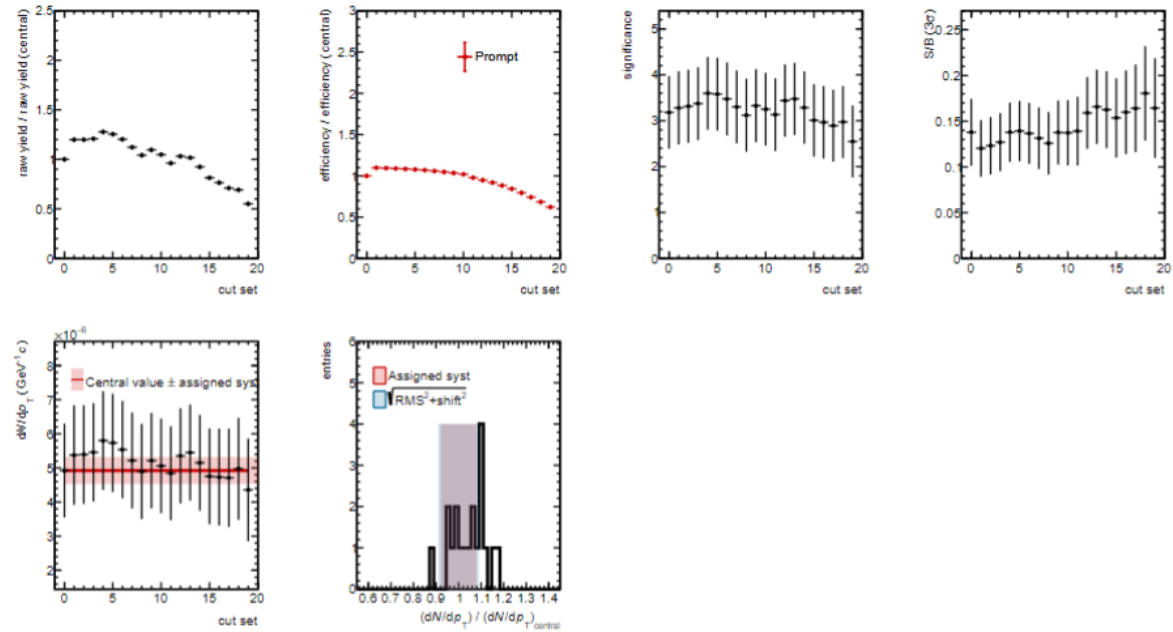
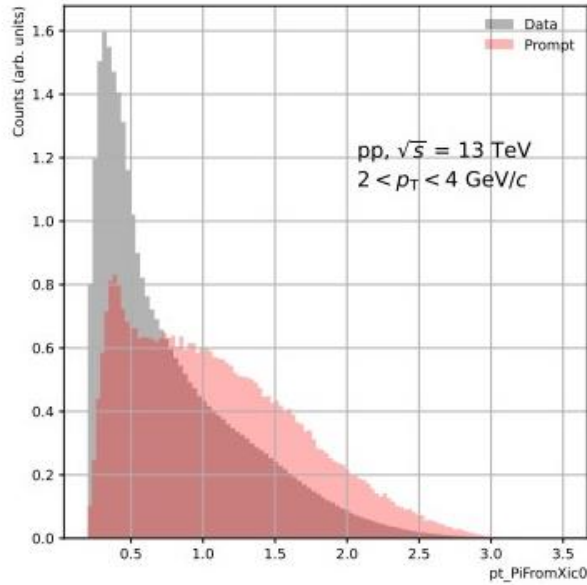


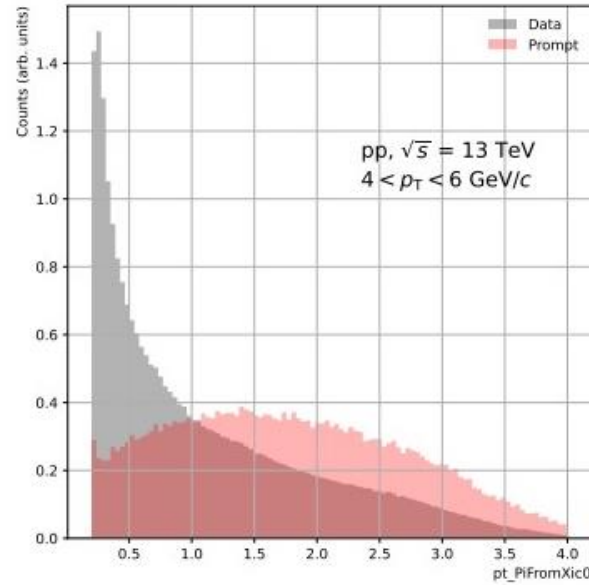
**Fig. 56:** The cut-variation studies for  $p_T$  bin 6GeV/c-8GeV/c and [30,100]V0M percentile multiplicity

# $p_T^\pi$ cut

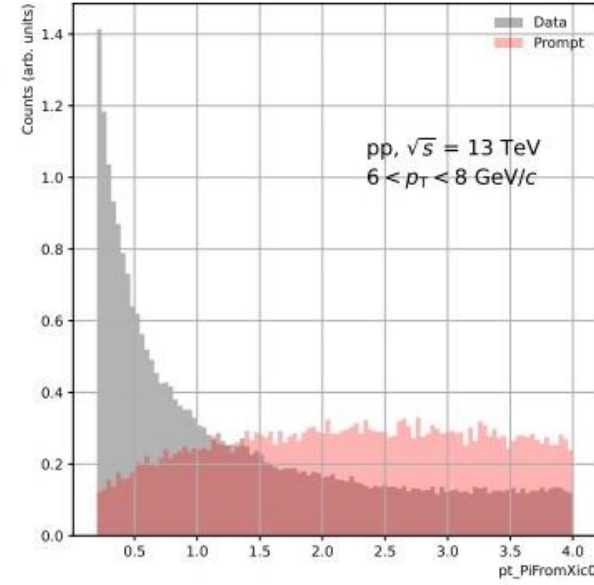
MB[0,100]



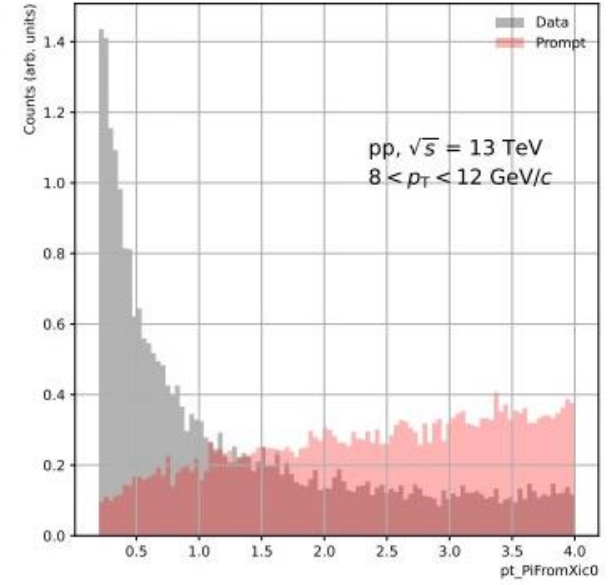
$2 < p_T < 4$  GeV/c



$4 < p_T < 6$  GeV/c



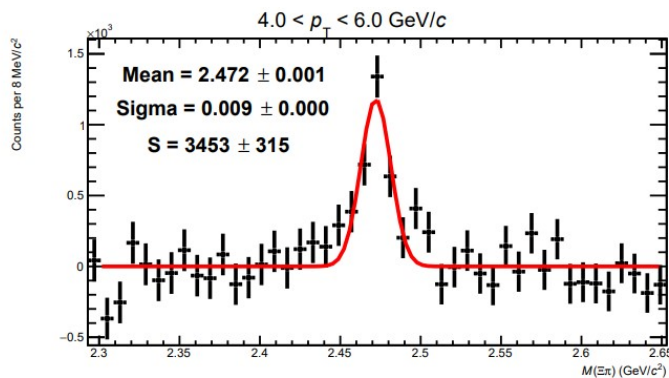
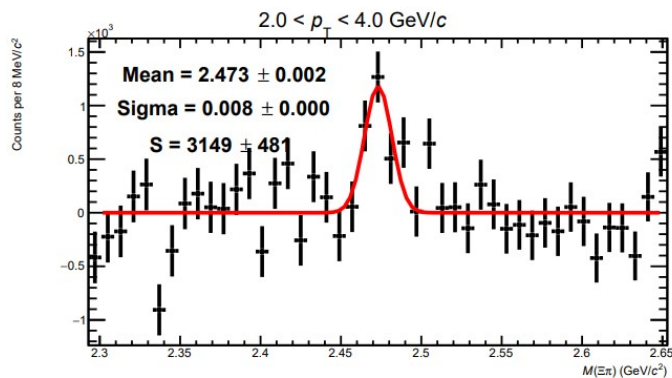
$6 < p_T < 8$  GeV/c



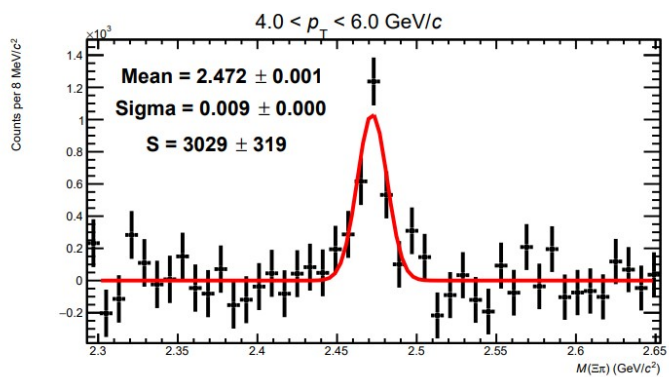
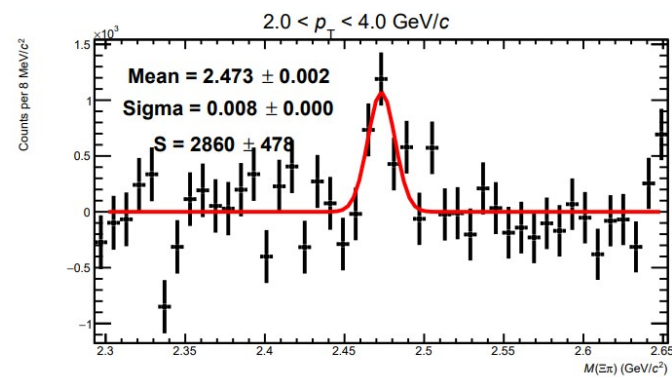
$6 < p_T < 8$  GeV/c

The normalized  $p_T^{\pi \leftarrow \Xi_c^0}$  distributions of MC signal and side band of data in each  $p_T^{\Xi_c^0}$  bin.

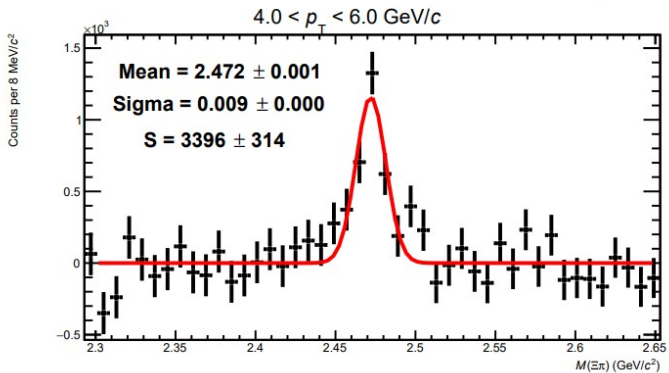
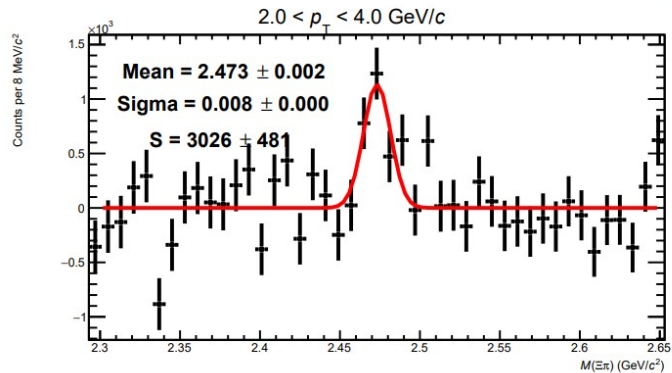
# Bkg fit function p\_V0M[0, 0.1]



Expo

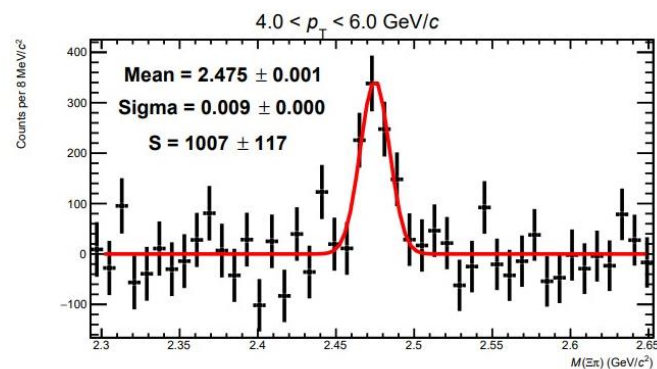
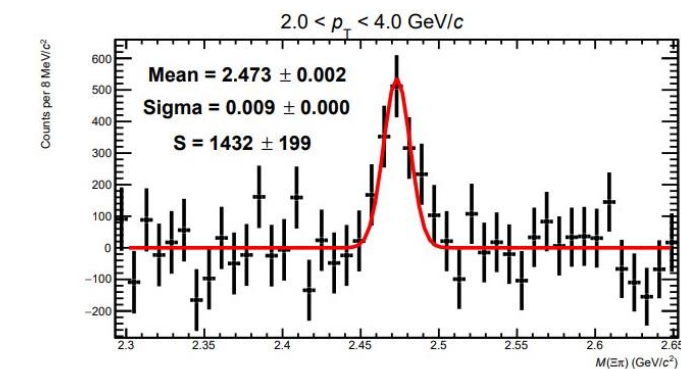


Pl02

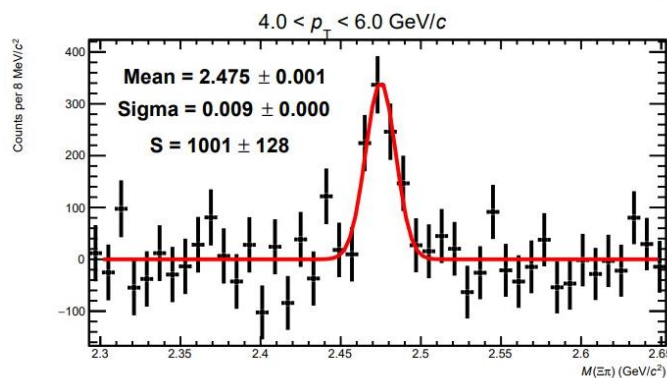
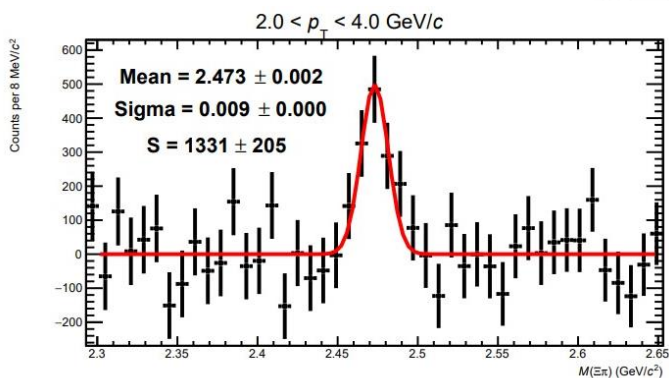


Pl01

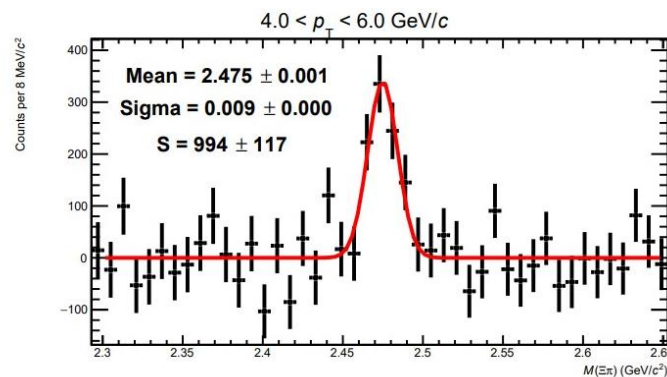
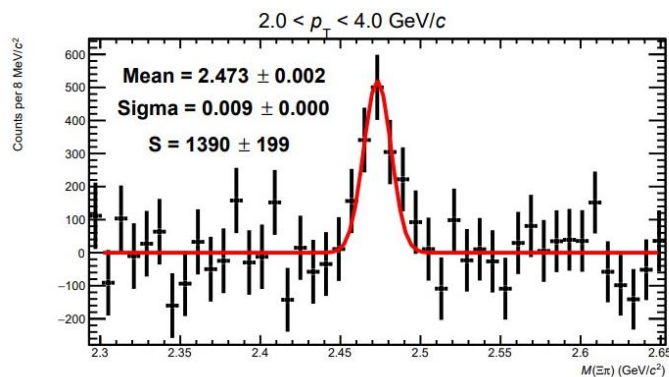
# Bkg fit function p\_V0M[0.1, 30]



Expo



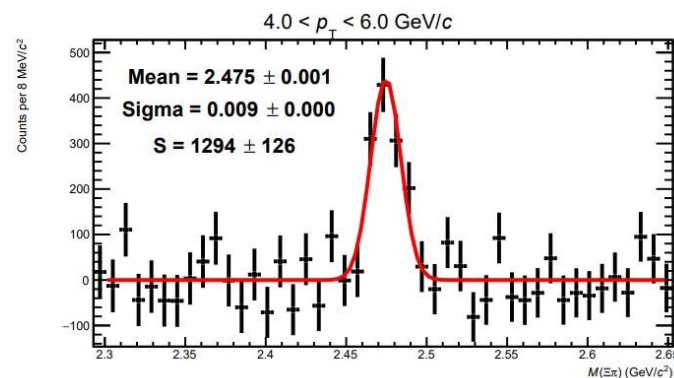
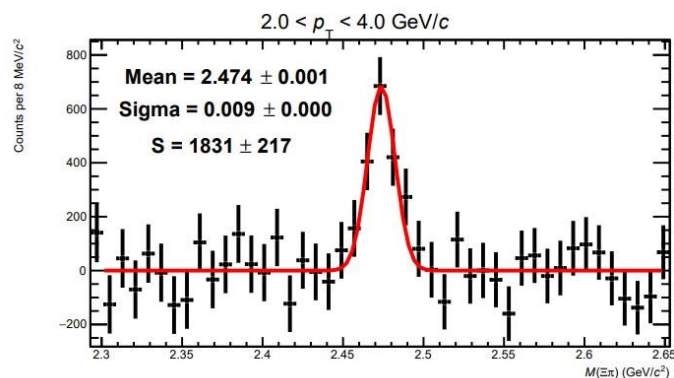
Pl02



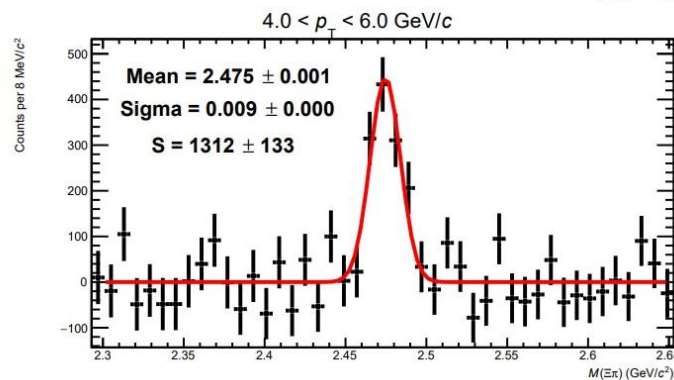
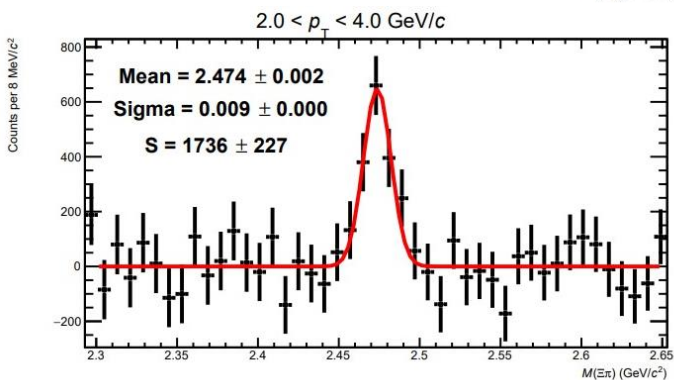
Pl01



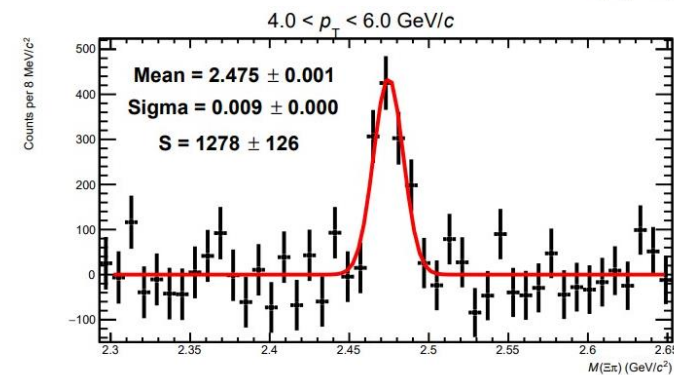
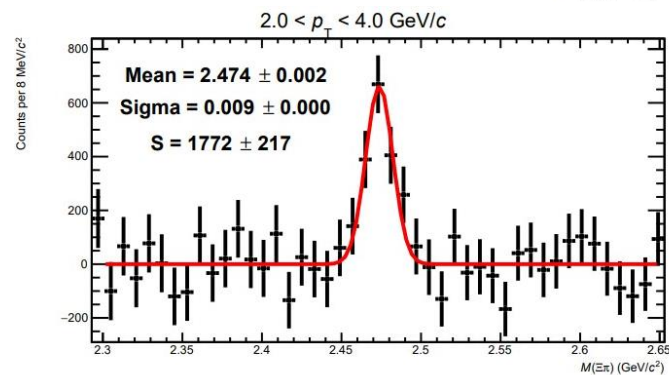
# Bkg fit function p\_V0M[0, 100]



Expo

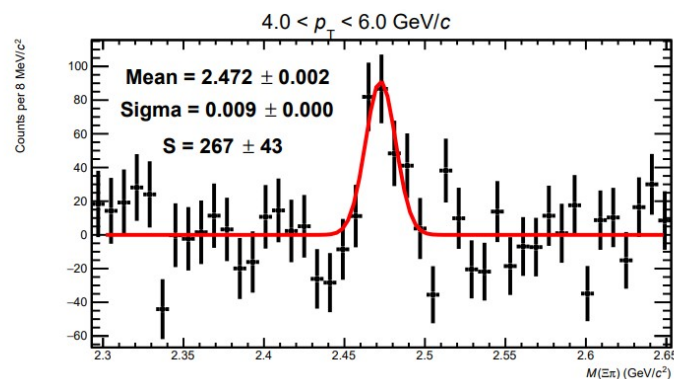
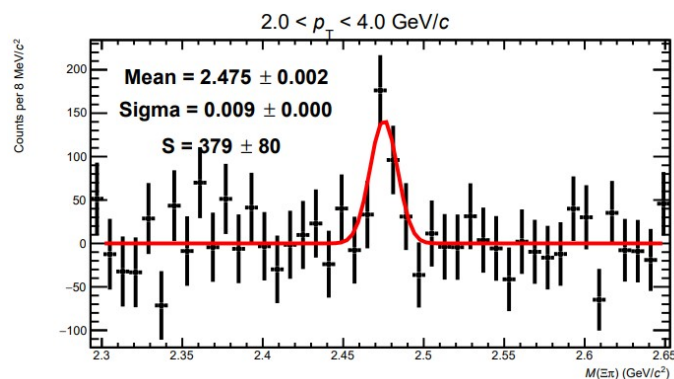


Pl02

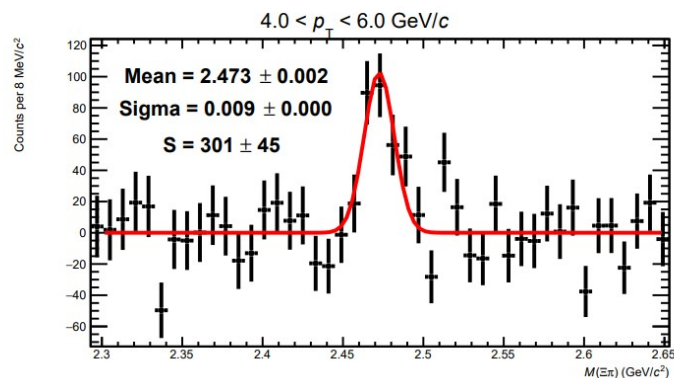
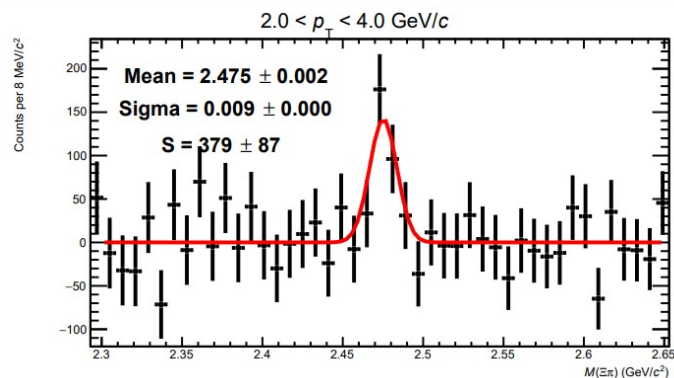


Pl01

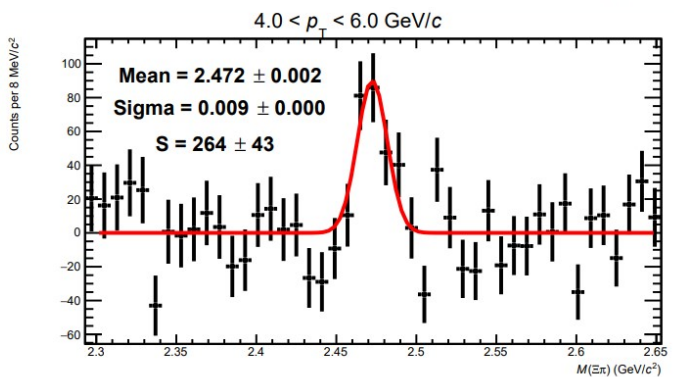
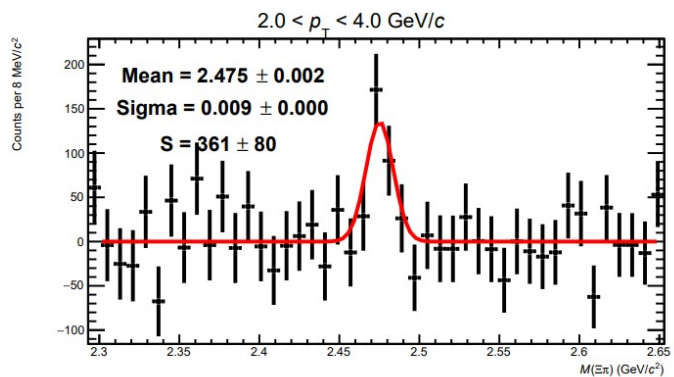
# Bkg fit function p\_V0M[30, 100]



Expo



Pl02



Pl01